The Effects of Vegetation on Stream Bank Erosion

Theresa M. Wynn

Dissertation submitted to the faculty of the Virginia Polytechnic Institute and State University in partial fulfillment of the requirements for the degree of

Doctor of Philosophy

In

Biological Systems Engineering

Saied Mostaghimi
James Burger
Theo Dillaha, III
Panayiotis Diplas
Conrad Heatwole

May 14, 2004
Blacksburg, Virginia

Keywords: stream bank erosion, riparian buffer, freeze-thaw cycling, desiccation cracking, submerged jet test device, root length density, subaerial processes, erodibility, critical shear stress

The Effects of Vegetation on Stream Bank Erosion

Theresa M. Wynn

Abstract

Riparian buffers are promoted for water quality improvement, habitat restoration, and stream bank stabilization. While considerable research has been conducted on the effects of riparian buffers on water quality and aquatic habitat, little is known about the influence of riparian vegetation on stream bank erosion.

The overall goal of this research was to evaluate the effects of woody and herbaceous riparian buffers on stream bank erosion. This goal was addressed by measuring the erodibility and critical shear stress of rooted bank soils in situ using a submerged jet test device. Additionally, several soil, vegetation, and stream chemistry factors that could potentially impact the fluvial entrainment of soils were measured. A total of 25 field sites in the Blacksburg, Virginia area were tested. Each field site consisted of a 2^{nd}-4^{th} order stream with a relatively homogeneous vegetated riparian buffer over a 30 m reach. Riparian vegetation ranged from short turfgrass to mature riparian forest. Multiple linear regression analysis was conducted to determine those factors that most influence stream bank erodibility and the relative impact of riparian vegetation.

Results of this research indicated woody riparian vegetation reduced the susceptibility of stream bank soils to erosion by fluvial entrainment. Riparian forests had a greater density of larger diameter roots, particularly at the bank toe where the hydraulic stresses are the greatest. These larger roots (diameters > 0.5 mm) provided more resistance to erosion than the very fine roots of herbaceous plants. Due to limitations in the root sampling methodology, these results are primarily applicable to steep banks with little herbaceous vegetation on the bank face, such as those found on the outside of meander bends.

In addition to reinforcing the stream banks, riparian vegetation also affected soil moisture and altered the local microclimate. While summer soil desiccation was reduced under deciduous

riparian forests, as compared to herbaceous vegetation, winter freeze-thaw cycling was greater. As a result, in silty soils that were susceptible to freeze-thaw cycling, the beneficial effects of root reinforcement by woody vegetation were offset by increased freeze-thaw cycling. Using the study results in an example application, it was shown that converting a predominately herbaceous riparian buffer to a forested buffer could reduce soil erodibility by as much as 39% in soils with low silt contents. Conversely, for a stream composed primarily of silt soils that are prone to freeze-thaw cycling, afforestation could lead to localized increases in soil erodibility of as much as 38%. It should be emphasized that the riparian forests in this study were deciduous; similar results would not be expected under coniferous forests that maintain a dense canopy throughout the year. Additionally, because dense herbaceous vegetation would likely not develop in the outside of meander bends where hydraulic shear stresses are greatest, the reductions in soil erodibility afforded by the herbaceous vegetation would be limited to areas of low shear stress, such as on gently sloping banks along the inside of meander bends.

As the first testing of this type, this study provided quantitative information on the effects of vegetation on subaerial processes and stream bank erosion. It also represents the first measurements of the soil erosion parameters, soil erodibility and critical shear stress, for vegetated stream banks. These parameters are crucial for modeling the effects of riparian vegetation for stream restoration design and for water quality simulation modeling.

Grant Information

Funds for this research were provided by Grant No. U-915555-01-0 under the Science to Achieve Results (STAR) program of the US Environmental Protection Agency, Office of Research and Development, National Center for Environmental Research; the American Association of University Women Selected Professions Fellowship; the P.E.O. Scholars Award; the Virginia Tech General Electric Fund Scholars Program; the Soil and Water Conservation Society Kenneth E. Grant Research Scholarship;, the American Water Resources Association Richard A. Herbert Memorial Education Scholarship; the Gene and Ina Mae James Graduate Scholarship; the Waste Policy Institute Graduate Fellowship; and the Virginia Water Resources Center William R. Walker Graduate Research Fellowship.

Dedication

I wish to dedicate this work to my guys, Benjamin and Jeffrey Wynn, and to remember those who passed during its development, including Ruth and Paul Schatzle, Johanna Gidley, Sherry Schatzle, Olga and John Sloboda, and Bernard Gidley.

“The difficulty lies not in the new ideas, but in escaping from the old ones.”

- John Maynard Keynes

Acknowledgements

I would like to thank my major professor, Saied Mostaghimi, for all his support and guidance throughout my dissertation program. I would also like to thank Jim Burger, Theo Dillaha, Panos Diplas, and Conrad Heatwole for their support and input. I am incredibly grateful to all those who assisted with the extensive field and laboratory work for the "Epic Project," including Charles Karpa, Jan Carr, Jeff Wynn, and Julie Jordan, as well as Joe Deal, Adam Faulkner, Adrian Harpold, Nyeema Harris, Marc Henderson, Leigh-Anne Henry, Leslie Johnson, Candice Piercy, Sheila Ranganath, and Meghan Siewers. Thank you for suffering through bad weather, equipment breakdowns, picking roots, and mud pies with me. Lastly, none of this research would have happened without the generosity and cooperation of numerous private landowners. Many thanks go to Bob Adams, the Blacksburg Country Club, Paul Bowyer, Carl Cirillo, Mark Cook, Tammy Decatur, Earl Frith, Joyce Graham, Chuck and Margie Harris, Mark and Linda McCann, Frank Quinn, Bob Ross, the Town of Blacksburg, Allen Sisson, and Jim Washington for allowing this research to be conducted on their property. I am particularly grateful to Earl Frith for loaning me his ATV, without which I would have had several long, cold, muddy hikes during the winter of 2003.

I would also like to acknowledge the love and support of may family. I want to thank my guys, Benjamin and Jeffrey Wynn, for enduring the mud, the poison ivy, and the days I couldn't play with you. I would also like to thank my parents, Susan and Larry Gidley, for the many hours of long distance listening and babysitting a sick grandchild. Thank you for your years of support in its multiple forms. Many thanks also go to Carol and Walter Wynn, for their encouragement and for filling in when I had to be gone. My family is a blessing beyond measure.

Table of Contents

List of Tables

List of Figures

List of Abbreviations and Symbols

ΔT ..... freezing point depression
γ ..... unit weight of water
ρ ..... Spearman's rho
σ ..... standard deviation of soil grain size
σ_{NT} ..... standard deviation of soil grain size
τ ..... Kendalls correlation coefficient
τ_c ..... soil critical shear stress
$\tau_{c,NT}$ ..... normalized and transformed soil critical shear stress
τ_f ..... applied fluvial shear stress
τ_o ..... maximum applied shear stress
μS ..... microsemin
%clay ..... soil clay content
%sand ..... soil sand content
a ..... fitted coefficient
ADF ..... average duration frozen
ADF_{NT} ..... normalized and transformed average duration frozen
AS ..... aggregate stability
AS_{NT} ..... normalized and transformed aggregate stability
ASAE ..... American Society of Agricultural Engineers
ASCE ..... American Society of Civil Engineers
ASTM ..... American Society for Testing and Materials
b ..... fitted exponent
BD ..... soil bulk density
BD_{NT} ..... normalized and transformed soil bulk density
BMP ..... best management practice
BRLD ..... big root length density
BRVR ..... big root volume ratio
$BRVR_{NT}$ ..... normalized and transformed big root volume ratio
BSA ..... basal stem area
BSA_N ..... normalized basal stem area
C ..... jet test nozzle coefficient
C_d ..... jet diffusion constant
Ca ..... calcium
CL ..... clay loam
d_o ..... jet test nozzle diameter
D ..... root diameter
D_{50} ..... median soil diameter
$D_{50,NT}$ ..... normalized and transformed median soil diameter
D_r ..... dispersion ratio
$Degrees_N$ ..... normalized degrees from north
$Depth_N$ ..... normalized average baseflow stream depth
E ..... erosion rate

E_i ..... initial erosion rate
EC ..... electrical conductivity
$Elev_N$ ..... normalized site elevation
ELx ..... East Fork of the Little River Site x
FRLD ..... fine root length density
$FRLD_{NT}$ ..... normalized and transformed fine root length density
FTC ..... freeze-thaw cycling
FTC_{NT} ..... normalized and transformed freeze-thaw cycling
FTCs ..... freeze-thaw cycles
Grass ..... grass dry biomass
$Grass_N$ ..... normalized grass dry biomass
h ..... jet test pressure head
H_e ..... jet maximum scour depth
H_i ..... jet initial height above soil surface
H_p ..... jet test core length
hr ..... hour
K_d ..... soil erodibility coefficient
$K_{d,NT}$ ..... normalized and transformed soil erodibility coefficient
K_f ..... freezing point depression constant for water
KIF ..... potassium intensity factor
KIF_{NT} ..... normalized and transformed potassium intensity factor
LS ..... loamy sand
m ..... soil solution molality
M ..... molarity
MC ..... soil antecedent moisture content
MC_{NT} ..... normalized and transformed soil antecedent moisture content
MDF ..... median duration frozen
NRx ..... North Fork of the Roanoke River Site x
NRCS ..... Natural Resources Conservation Service
O ..... clay alumina octahedra sheet
OC ..... soil organic carbon content
OC_{NT} ..... normalized and transformed soil organic carbon content
PCA ..... principle components analysis
PI ..... plasticity index
PSA ..... particle size analysis
PW ..... pore water salt concentration
R ..... channel hydraulic radius
RAR ..... root area ratio
RDAM ..... relative difference between average and median freezing durations
$RDAM_{NT}$ ... normalized and transformed rel. diff. between average and median freezing durations
RLD ..... root length density
RVR ..... root volume ratio
Sand ..... soil sand content
$Sand_{NT}$ ..... normalized and transformed soil sand content
S ..... channel energy grade line slope
S_v ..... soil shear strength

SAP ..... subaerial processes
SAR ..... sodium adsorption ratio
S:C ..... soil silt:clay ratio
$S:C_{NT}$ ..... normalized and transformed soil silt:clay ratio
S+C ..... sum of soil silt and clay fractions
$S+C_N$ ..... normalized sum of soil silt and clay fractions
SCx ..... Sinking Creek Site x
SCV ..... shrub crown volume
SG ..... soil specific gravity
SG_{NT} ..... normalized and transformed soil specific gravity
SiL ..... silty loam
$Silt_N$ ..... normalized soils silt content
SL ..... sandy loam
SRx ..... South Fork of the Roanoke River Site x
ST ..... soil temperature
STx ..... Stroubles Creek Site x
SWEC ..... ratio of soil to water specific electrical conductivity
SWP ..... soil water potential
SWpH ..... ratio of soil pH to water pH
$SWpH_{NT}$ ..... normalized and transformed ratio of soil pH to water pH
t ..... time of scour
T ..... clay silica tetrahedra sheet
TCx ..... Toms Creek Site x
TD ..... tree density
TDF ..... total duration frozen
TGC ..... total groundcover dry biomass
TMDL ..... total maximum daily load
TS ..... soil total salt concentration
TS_{NT} ..... normalized and transformed soil total salt concentration
U_o ..... jet velocity in core
VFRLD ..... very fine root length density
VIF ..... variance inflation factor
WDC ..... wetting-drying cycling
WDCs ..... wetting-drying cycles
WGC ..... woody groundcover dry biomass
WGC_N ..... normalized woody groundcover dry biomass
$Width_N$ ..... normalized average stream baseflow width
WT ..... stream water temperature
WT_{NT} ..... normalized and transformed stream water temperature
x ..... depth down stream bank
y ..... total root length density at depth x

Chapter 1. Introduction

1.1. Introduction

Sediment is a primary cause of water quality impairment, causing roughly $16 billion in damage annually in North America (USEPA, 2002; ARS, 2003). While considerable effort has been directed toward developing best management practices (BMPs) to reduce erosion from agricultural and urban lands, another major source of sediment, stream channel erosion, has largely been ignored. Studies have shown that sediment from stream banks can account for as much as 90% of watershed sediment yields (Kirkby, 1967; Grissinger et al., 1981a; Roseboom and Russell, 1985; Trimble, 1997a; Lawler et al., 1999; Prosser et al., 2000). In addition to water quality impairment, stream bank erosion impacts floodplain residents, riparian ecosystems, bridges, and other stream-side structures (ASCE, 1998a). Bank erosion rates of 1.5 - 1100 m/year have been documented (Simon et al., 2000). In 1981, the U.S. Army Corps of Engineers estimated that 575,000 stream bank miles were actively eroding, requiring an average annual treatment cost of $1.1 billion (USACE, 1981).

Riparian buffers are a recognized BMP for water quality improvement and stream restoration (Dillaha et al., 1989; Lowrance et al., 1995; Correll, 1996; Daniels and Gilliam, 1996). A riparian buffer is commonly defined as a band of vegetation adjacent to a body of water that forms the transition between aquatic and upland environments (Palone and Todd, 1997). In the eastern U.S., riparian vegetation ranges from grasses and forbs to shrubs and mature forests. Research has shown that grass and forested riparian buffers are effective at removing contaminants from overland flow and shallow groundwater (Lowrance et al., 1995). Forested buffers are also critical for maintaining aquatic ecosystems in eastern streams (Palone and Todd, 1997).

In addition to water quality and habitat benefits, riparian vegetation has a significant impact on stream stability and morphology (Mosley, 1981; Hey and Thorne, 1986; Gregory and Gurnell, 1988; Thorne and Osman, 1988; USACE, 1994; Abernethy and Rutherfurd, 2000). As such, it has become an integral part of stream restoration designs (Henderson, 1986; Shields, Jr. et al., 1995; Jennings et al., 1999). While the importance of vegetation in stream bank stability is widely acknowledged, the impacts are complex, poorly understood, and have yet to be quantified

(Mosley, 1981; Murgatroyd and Ternan, 1983; Hickin, 1984; Heede and Rinne, 1990; ASCE, 1998a; Abernethy and Rutherfurd, 2000; Thorne et al., 1997). Current stream restoration designs are based on empirical methods and standardized practices (Gregory and Gurnell, 1988; O'Laughlin, 1995; FISRWG, 1998; Jennings et al., 1999; VeriTech, Inc., 1999; Hession, 2001). A better understanding of the effects of vegetation on the processes involved in stream bank retreat is necessary for improved stream restoration design and riparian management (Abernethy and Rutherfurd, 1998). As Bohn (1989) stated "…by understanding the processes which weaken stream banks, land managers can develop streamside management strategies which reduce stream bank vulnerability and favor functional stability."

Stream restoration designs also need to be assessed for their long-term success, particularly in the face of future landuse changes (Horwitz et al., 2000). Existing models of stream morphology provide little assistance in the assessment of stream restoration projects because they do not consider the effects of vegetation (ASCE, 1998b). Additionally, as states are required to develop management plans with Total Maximum Daily Loads (TMDLs) for listed impaired waters, there will be a need to quantify all significant sources of sediment within watersheds and to determine the effect of proposed controls.

Vegetation type also plays a key role in channel morphology (Hey and Thorne, 1986; Hession, 2001). Several researchers have noted that streams were 2 - 2.5 times wider with forested riparian buffers than with grass buffers (Zimmerman et al., 1967; Clifton, 1989; Sweeney, 1992; Davies-Colley, 1997; Trimble, 1997b; Hession et al., 2000). This information has prompted some researchers to predict that watershed afforestation may lead to increased sediment yields (Murgatroyd and Ternan, 1983; Smith, 1992; Davies-Colley, 1997; Trimble, 1997b; Davies-Colley, 2000; Lyons et al., 2000) and that stream sediment yields could be reduced by converting riparian forests to grass (Trimble, 1997b). Alternatively, others have shown that forested streams are narrower than streams with herbaceous buffers (Gregory and Gurnell, 1988; Rosgen, 1996). A study in British Columbia determined major bank erosion was 30 times more prevalent on nonforested versus forested meander bends (Beeson and Doyle, 1995). In a study following the 1993 Kansas floods, Geyer et al. (2000) showed that areas with herbaceous buffers experienced an average of 24 m of bank erosion while areas with forested buffers experienced soil deposition. Hession (2001) hypothesized these conflicting findings on the effects of vegetation on channel form are the result of site-specific differences in watershed

characteristics, such as vegetation density and type, soils, flow regimes, slopes, geology, stream size, and disturbance history. Ultimately, further studies are necessary to evaluate the impact of vegetation type on stream morphology for effective stream and river management (Mosley, 1981; Gregory and Gurnell, 1988; Heede and Rinne, 1990; Thorne, 1990; Abernethy and Rutherfurd, 1998; ASCE, 1998a; Horwitz et al., 2000; Lyons et al., 2000; Hession, 2001; Simon and Collison, 2001).

1.2. Goals and Objectives

The overall goal of this research is to compare the effects of woody and herbaceous vegetation on stream bank erosion. This research is intended to evaluate the effects of vegetation on the susceptibility of stream bank material to fluvial entrainment. The results of this research will provide quantitative information for the design of stream restoration projects, will assist with the development of sediment TMDLs, and will provide guidance to watershed managers in the selection of riparian vegetation. Specific objectives include the following:

1. Quantify root-length density with depth in stream banks as a function of riparian buffer vegetation type and density;
2. Determine the effect of vegetation type on freeze-thaw and desiccation activity in stream bank soils; and
3. Use in situ erodibility measurements to evaluate the relative effects of vegetation type and root-length density on the erodibility of stream banks.

1.3. Study Design

A stable stream is one where the flow regime and sediment supply are in a state of quasi-equilibrium over a period of decades or centuries (Schumm and Lichty, 1965). These systems are often referred to as “graded” or “in regime” (Mackin, 1948; Leopold and Maddock, 1953; Wolman, 1955; Leopold et al., 1964; Ackers, 1992; ASCE, 1998a). While stream bank erosion may occur in stable streams, particularly on the outside of meander bends, this erosion is balanced by deposition on the opposite bank, such that graded streams maintain their channel form over long periods of time. Several models are used to predict the geometry of stable streams for engineering design. Examples include empirical (regime and power law), extremal hypothesis, or mechanistic (tractive force) methods (ASCE, 1998a). Recent research and modeling efforts in the design of stable stream channels have utilized the mechanistic tractive

force method to evaluate stream stability (Osman and Thorne, 1988; Simon et al., 1999; Langendoen, 2000). This research assumes this mechanistic tractive force model to address the role of vegetation in stream bank stability by assessing the impact of riparian vegetation on two processes involved in stream bank retreat, subaerial processes and bank erosion (fluvial entrainment).

Twenty-five field sites were established along streams near the Town of Blacksburg in southwest Virginia ($37^{o}15'$ N, $80^{o}25'$ W; Figure 1.1). Each field site consists of a 2^{nd}-4^{th} order stream with a relatively homogeneous vegetated riparian buffer over a stream reach of 30 meters. The study focused on a 10 m wide buffer area, as measured from the edge of the baseflow water level. Average baseflow depths were 20 - 50 cm, while bank exposure ranged from 65 cm to 225 cm and bank angles were 30^{o}-90^{o}. Baseflow channel widths varied from 3 m to 24 m, with drainage areas of 9 - 322 km^2. Bed materials ranged from sand to boulders. The riparian vegetation varied from short turfgrass to mature forests, representing the full range of possible vegetation types.

This area lies in the Appalachian Mountains in southwestern Virginia and the climate is typical of temperate mountain regions. Elevations range from 350 m to 900 m NGVD29 and average annual rainfall is about 1100 mm. Rainfall has a relatively even distribution throughout the year, although slightly more precipitation occurs in spring and droughts are common in late July and August. Individual site information is detailed in Appendix A with photographs of each site.

To address the research objectives, three separate studies were undertaken. The first study measured root density and distribution in riparian stream banks as a function of riparian vegetation type and density, while the second study evaluated the effects of riparian vegetation on stream bank soil temperature (ST) and moisture regimes. The third and final study quantified stream bank soil erodibility and critical shear stress in situ. The effects of aboveground vegetation density, root density, soil freeze-thaw cycling, and soil chemical and physical properties on stream bank erosion were evaluated. The methodology, results, and discussion for each of the studies is presented in separate chapters.

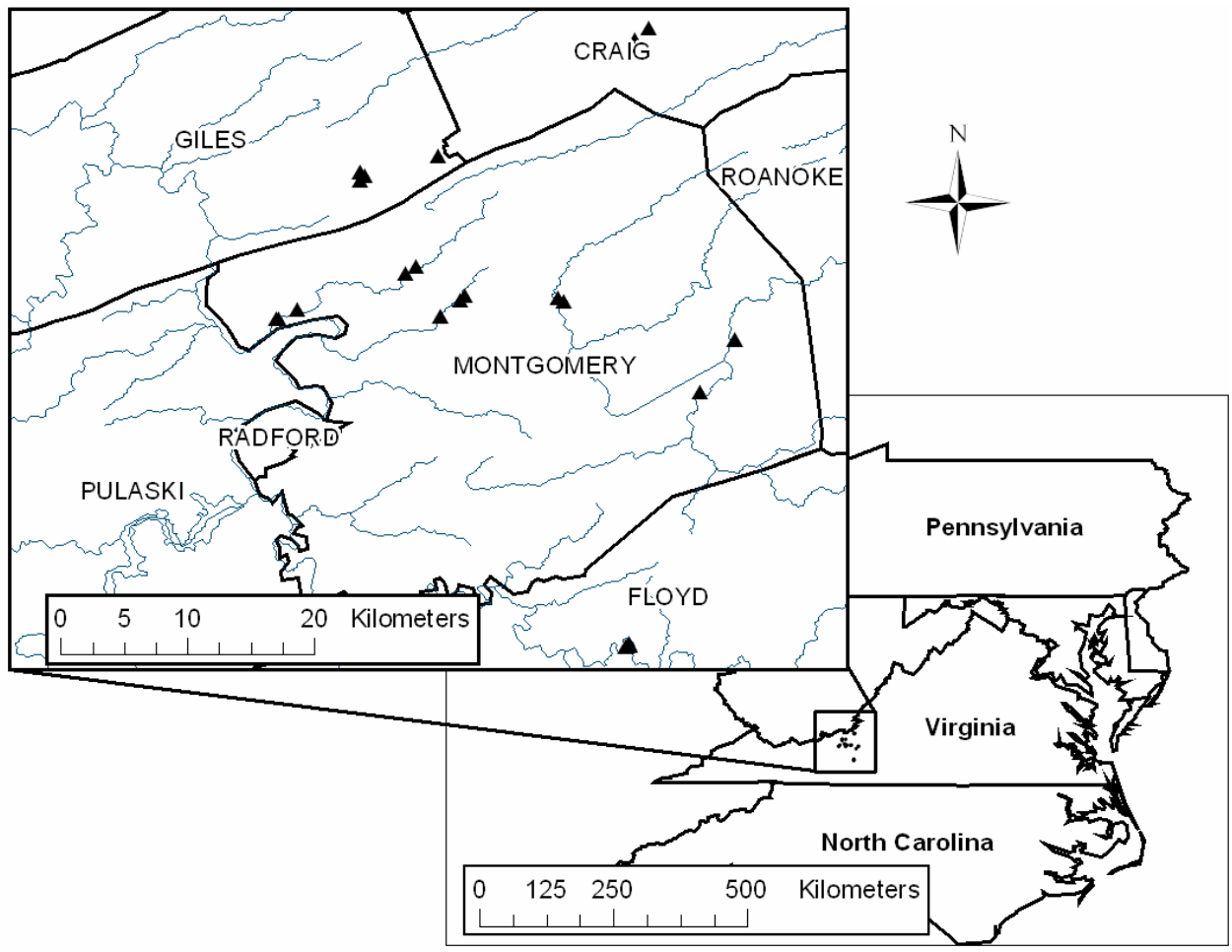

Figure 1.1. Location of research field sites, southwestern Virginia, USA.

Chapter 2. Review of Stream Bank Retreat

Changes in watershed landuse, river regulation, or channel engineering may change stream flow and/or sediment regimes and these may trigger instabilities in stream form. Stream bank erosion occurs by a combination of three processes: subaerial processes, fluvial entrainment, and mass wasting (Lawler, 1992; Lawler, 1995). Each of these processes is discussed in the following chapter. Also considered are the effects of vegetation on these three processes and methods to model stream bank erosion.

To provide clarity for the following discussions, the author adopted the terminology proposed by Lawler et al. (1997). Specifically, the terms “erosion” and "fluvial entrainment" are used to describe the detachment, entrainment, and removal of individual soil particles or aggregates from the stream bank face by the hydraulic forces occurring during flood events. The phrases “bank failure” or "mass wasting" denote the physical collapse of all or part of the stream banks as a result of geotechnical instabilities. Bank erosion and bank failure commonly work in concert to produce “bank retreat” or the net recession of the stream bank. Two additional terms, soil “erodibility” and “critical shear stress” describe, respectively, the ease with which soil is removed from the bank face and the hydraulic shear stress at which significant erosion is initiated. As will be discussed in the following sections, these parameters are used in the excess stress equation and are primarily dependent on soil properties (Hanson and Simon, 2001).

2.1. Subaerial Processes

Subaerial processes (SAP) are climate-related phenomena that serve to reduce soil strength (e.g. frost heave, soil desiccation; Thorne, 1982). Controlled mainly by climatic conditions, SAP are largely independent of flow. They dominate stream bank retreat in the upper reaches of river systems, delivering soil directly to the stream channel and making the banks more vulnerable to flow erosion by reducing the packing density of soils and destroying imbrication (Thorne and Tovey, 1981; Abernethy and Rutherfurd, 1998). Measured average erosion rates due exclusively to SAP range from 13 mm/yr (Prosser et al., 2000) to 40 mm/yr with peaks as high as 181 mm/yr (Couper and Madock, 2001). Subaerial processes are

sometimes described as “preparatory processes” as they increase soil erodibility (Wolman, 1959; Lawler, 1993).

2.1.1. Soil Desiccation

Contrasting views exist regarding the effects of desiccation on soil erodibility. Several researchers have shown that drier soils are more resistant to fluvial entrainment (Wolman, 1959; Knighton, 1973; Hooke, 1979). Soil desiccation has been shown to increase soil strength: Nearing et al. (1988) stated soil suction increases soil stability by increasing the effective stress in soils. Soil drying can also cause soil cementation due to the precipitation of calcium carbonates, silica, gypsum, or iron oxides (Lehrsch, 1998).

Alternatively, soil desiccation can decrease soil strength. Stream bank desiccation creates peds and crumbs, which have little resistance to erosion, and can create conditions for soil slaking (Figure 2.1; Thorne, 1982; Robinson et al., 2000). Slaking is the bursting of soil aggregates in response to a buildup of pore air pressure when soils are rapidly wetted. Soil desiccation can also cause vertical tension cracks which reduce the structural strength of the stream bank (Thorne, 1982). Cracks as wide as 125 mm and as deep as 200 mm have been reported (Greenway, 1987; Coppin and Richards, 1990). These cracks increase soil permeability and may create higher pore water pressures which reduce bank stability (Greenway, 1987; Davidson et al., 1991). Knighton (1973) noted that cycles of wetting and drying influence bank erodibility more than the actual bank material composition. Shiel et al. (1988) showed that repeated cycles of wetting and drying decreased aggregate size in clay soils. This reduction in aggregate size makes the soil more susceptible to entrainment during storm events. In arid climates with high clay content soils, soil desiccation alone can dominate bank retreat (Greene, 1999; Prosser et al., 2000).

2.1.2. Soil Freeze-Thaw Cycling

Multiple cycles of freezing and thawing (5-10) decrease aggregate stability and soil shear strength, break soil peds apart, and make soil more susceptible to erosion (Mostaghimi et al., 1988; Thorne, 1990; Eigenbrod, 2003). The freezing process causes a migration of soil water toward the freezing front and can lead to the formation of large ice crystals which decrease soil density (Branson et al., 1996). This effect is particularly pronounced in fine grained soils: the pore sizes in silty soils are small enough to create a gradient in soil suction, but large enough to

allow relatively rapid water movement toward the freezing front (Gatto and Ferrick, 2002). Soils with a silt-clay content greater than 20% are considered "frost-susceptible" (Matsuoka, 1996). Frost susceptibility is also a function of vegetative cover, initial soil temperature, air temperature regime, solar exposure, soil temperature gradient, rate of heat loss, mobility of soil water, depth to the water table, overburden stress and soil density (Jumikis, 1962; Chamberlain, 1981). In south-central Idaho, as many as 30-40 freeze-thaw cycles (FTCs) can occur in one winter. Freezing periods on the order of hours to weeks can occur (Hershfield, 1974).

The effects of frost on soil aggregate stability was investigated by Mostaghimi et al. (1988) using a rainfall simulator. Samples of loam, silt loam, and clay loam soils were frozen at six different moisture contents, ranging from near saturation to a soil water suction of 15 atm. Both slow and quick freezing rates were used to create zero, one, three, or six freeze-thaw cycles (FTCs). The samples were subsequently exposed to a simulated brief, intense rainfall event (6.4 cm/hr for 10.5 minutes). Aggregate stability for the unfrozen controls, the frozen controls, and the frozen and impacted samples was measured using wet sieving. Results of the study showed that the effects of raindrop impact on soil aggregate stability was greater that the effects of FTC. The moisture content at the time of freezing affected aggregate stability: each soil had an optimum moisture level at which the effects of FTC was minimized. While aggregate stability decreased with increasing FTC for the loam and the clay loam, it increased for the silt loam after one to three FTCs. Following six FTCs, silt loam aggregate stability ultimately decreased.

Asare et al. (1997) evaluated the effects of freeze-thaw cycling on the strength of remolded samples of silt loam, clay loam, and loamy sand soils. They exposed the samples to one, three, and six FTCs and determined that soil shear strength, as measured by a cone penetrometer, decreased with increasing FTC.

Lehrsch (1998) showed that low numbers of FTCs may act to increase aggregate stability. In a laboratory study of four U.S. soils, Lehrsch determined the wet aggregate stability of each soil at two depths (0-15 mm and 15-30 mm) following one to four FTCs at field capacity. Results of the study indicated wet aggregate stability increased following two to three FTCs. This effect was less pronounced for the 15-30 mm layer. The author concluded occasional freezing of moist soil may improve soil structure.

Figure 2.1. Soil cracking due to desiccation at site ST3. Camera lens cap is 5.5 cm in diameter.

Oztas and Fayetorbay (2003) studied four soils common to Turkey and evaluated the wet aggregate stability of three different size groups (0-1 mm, 1-2 mm, 2-4 mm) as a function of moisture content at freezing, freezing temperature, and number of FTCs (three, six or nine FTCs). Following freezing, aggregate stability decreased 13.8% to 57.7%. Average decreases in aggregate stability ranged from 28.6% for a clay soil to 51.7% for a clay loam soil. In general, the effects of FTC appeared less for soils with poor structure than for those with good structure. The moisture content at the time of freezing had a strong effect on changes in aggregate stability: mean aggregate stability for soils frozen at 90% of saturation was 40% less than that of soils frozen air dry. Differences in freezing temperature were also significant. Soils frozen at -18^{o}C had 10% lower aggregate stability than soils frozen at -4 ^{o}C. Increases in the number of FTC did not produce a consistent effect on aggregate stability. Mean aggregate stability increased as the

number of FTCs increased from three to six, but decreased with greater than six FTCs. This supports findings by Lehrsch et al. (1991) and Lehrsch (1998) that FTC increases aggregate stability for only a few FTCs and then subsequently decreases.

In addition to producing changes in soil strength, SAP may contribute soil directly to the stream. The contribution of SAP to bank erosion, independent of fluvial entrainment, was measured over 15 months in the River Arrow watershed in central England (Couper and Maddock, 2001). Bank retreat was measured using a grid of 284 erosion pins. The average rate of retreat by SAP was 32.6 mm/yr, with a range of 0-181 mm/yr. The authors noted that, while erosion occurred throughout the year, it was most severe during the winter. Correlating retreat rates with meteorological data, a significant relationship between retreat activity and the number of frost days per fortnight was found. The authors also noted that the highest retreat rates were found at sites with high soil silt-clay contents (Couper and Maddock, 2001).

These results were confirmed in a subsequent laboratory study on the effects of soil silt-clay content on subaerial processes (Couper, 2003). Both remolded and undisturbed soil samples with silt-clay contents of 30-75% were subjected to either 30 FTCs or 70 wetting-drying cycles (WDCs). Changes in sample dimensions and the total mass and aggregate size of eroded soil were measured. While the WDCs did not affect expansion and contraction of the soil blocks, the mass of soil lost from the soil block as a result of WDC increased exponentially with increasing clay content. Undisturbed field samples had a higher eroded mass and larger eroded aggregates than remolded samples, indicating that remolded samples may not replicate field conditions due to a lack of existing cracks and other weaknesses. Freeze-thaw cycling had a significant impact on the degradation of the soil blocks. While no significant relationship was determined between dimensional changes and the soil silt-clay content, there was positive correlation of mass eroded and aggregate size to silt-clay content. The greatest increase in these parameters was seen at silt-clay contents between 50% and 55%. These results indicate that the silt-clay content of soils does have a significant positive impact on SAP and that FTC produces greater soil degradation than WDC.

Soils that are high in loam are also susceptible to needle ice formation. Needle ice filaments form normal to the soil surface and are typically 1 mm^2 in cross section, reaching lengths up to 8-10 cm (Outcalt, 1971). These thin filaments of ice weaken the bank surface and

may dislodge individual soil particles, causing soil to fall into the stream or collect at the bank toe (Lawler, 1993). Lawler (1993) estimated that bank retreat due to needle ice accounted for 32-43% of the total bank retreat measured along the River Ilston, West Glamorgan, UK.

Branson et al. (1996) conducted a laboratory study of needle ice formation using undisturbed soil blocks from a stream bank. They measured soil temperature (ST) and moisture content at the soil surface and at 1 cm depth. Their study showed that ice formation did not start until the soil surface temperature reached -1.5^{o}C, but, once started, ice formation continued as long as the ST remained below 0 ^{o}C. During needle ice formation, a constant flux of heat and moisture to the soil surface was maintained and the temperature at a 1 cm depth remained above 0 ^{o}C. If the air temperature decreased, or soil moisture was limited, then needle ice formation ceased and the freezing front moved down into the soil profile, freezing the soil water without ice segregation. Their study illustrates the interplay between soil cooling and soil moisture flux in determining the depth of soil freezing and the form of the soil ice.

2.1.3. The Significance of Subaerial Processes

Subaerial processes (SAP) are considered of secondary importance by some researchers (Thorne, 1982; Abernethy and Rutherfurd, 1998), while others consider them significant factors in bank retreat (Hooke, 1979; ASCE, 1998a; Couper, 2003). Thorne and Lewin (1979) studied bank retreat along the River Severn in Wales between September 1976 and April 1977. The stream banks consisted of cohesive soil overlying coarser noncohesive soil at the bank toe. Erosion pins were installed at 14 sections along a meander bend. Four of these sections were in areas the river had abandoned and so were not affected by river flow; these sections were considered a control and were used to compare SAP to other bank retreat processes. The authors noted that SAP produced significant retreat on steep, unvegetated banks. Average annual retreat rates of 15-25 mm/yr due to SAP alone were measured, with winter peaks of 30 mm/yr, and summer rates of only 12 mm/yr. During the winter, freezing loosened aggregates in the upper bank and removed interstitial sand in the coarser lower bank. This material collected in a talus slope at the bank toe and stabilized the upper bank. In comparison, fluvial entrainment of the lower bank frequently produced erosion rates greater than 350 mm/yr and as high as 600 mm/yr. Erosion rates of the upper bank due to fluvial entrainment were greatest in the winter but averaged only 28 mm/yr due to the higher resistance of the cohesive soil and the lower applied

shear stresses on the upper bank. The authors concluded fluvial entrainment and mass failure produced retreat rates an order of magnitude greater than SAP.

Prosser et al. (2000) measured bank erosion in an ephemeral gully with clayey cohesive soils and little vegetation in Tasmania, Australia for two years. Stream bank retreat was measured using erosion pins and a ground profiler. Stream bank STs, as well as stream stage and turbidity were also monitored. Bank retreat rates averaged 13 ± 2 mm/yr. The authors stated that bank erosion contributed significant quantities of sediment to the stream during the study period and that most of the bank erosion resulted from subaerial processes. Both summer soil desiccation and winter needle-ice formation created a layer of loose soil on the bank surface that was easily eroded, while the underlying clay soil remained resistant to fluvial entrainment. Even though erosion was greatest over the winter when stream flows were high, summer soil desiccation created spalling of the upper bank soils. This loosened material typically accumulated on the lower banks where it was later removed by winter flows. Hysteresis observed in the stream turbidity measurements may have been the result of supply limitation from the stream banks. The authors stressed that models of channel erosion based on excess shear stress would underestimate stream channel erosion in this case because the sediment load is controlled by the extent of soil degradation by SAP.

Based on field and laboratory studies, Couper (2003) postulated that the contribution of SAP to stream bank erosion may be underestimated because erosion by freeze-thaw cycling coincides with spring flood events. In a study of the fate of failed bank material, Wood (2001) noted that SAP accelerated the weathering and erosion of blocks of cohesive soil in the basal area of actively eroding stream banks in Goodwin Creek, Mississippi. Based on observation, Wood concluded the degradation by FTC and desiccation were equally significant. This contradicts studies by Couper and Maddock (2001) and Couper (2003), which indicate FTC contributes more to bank erosion than WDC.

2.2. Fluvial Entrainment

Fluvial entrainment is the direct removal of soil particles or aggregates from the stream bed or banks by flowing water (Thorne, 1982). The erodibility of noncohesive soils is a function of soil grain size distribution, shape, and density (Allen et al., 1999). Alternatively, the erosion of cohesive soils is extremely complex and is related to soil properties and test conditions

(Grissinger, 1982). Simply determining which soils are cohesive is difficult: repulsive and attractive forces exist in soils and the net force is often a function of both the physical and chemical properties of the soil. Soils with a plasticity index less than 10 are commonly classified as cohesionless, although this criterion is frequently inadequate in describing soil behavior (Hanson, 1991).

Considerable research has been conducted on the erosion of cohesive soils, but the results are often contradictory and few design data are available. Grissinger (1982) presented a comprehensive summary of previous research. Most studies were conducted using laboratory methods with small remolded samples. Test equipment has included straight and circular flumes, pinhole devices, rotating cylinders, disks and impellers, and submerged jet devices (Allen et al., 1999). These studies have shown that the fluvial entrainment of cohesive soils is determined by the soil structure and the interaction between the soil pore water and the eroding fluid (Heinzen, 1976). While noncohesive soils erode as individual grains, cohesive soils erode as aggregates; thus, interped bonding is also important (Grissinger, 1982; Thorne, 1982; Osman and Thorne, 1988; ASCE, 1998a; Langendoen, 2000). Additionally, the surface morphology of bank soils influences near bank hydraulic stresses and soil entrainment (Grissinger et al., 1981b; Grissinger, 1982). These two considerations suggest that laboratory studies using small remolded samples may not be applicable to field conditions. Indeed, research has shown that remolded soils have lower critical shear stresses and higher overall erosion rates than undisturbed samples (Heinzen, 1976; Arulanandan et al., 1980).

Since erosion is a surface phenomenon, and surface soils equilibrate quickly to changes in pore water pressure and solution chemistry, the erodibility of cohesive soil is affected by test conditions. The temperature of the eroding fluid, the sample antecedent moisture content, the rate of sample wetting, and the suspended solids concentration and chemistry of the eroding fluid influence soil erodibility (Grissinger, 1982; Thorne, 1982; Allen et al., 1999). Soil bulk properties, such as vane shear strength, compressive strength and dry unit weight, are not good indicators of the erosion potential of cohesive soils (Arulanandan et al., 1980).

2.2.1. The Effects of Soil Properties on Fluvial Entrainment

A number of soil parameters influence the susceptibility of a cohesive soil to erosion, including grain size distribution, soil bulk density, clay type and content, organic matter content,

and soil pore water content and chemistry (Arulanandan et al., 1980; Grissinger, 1982; Osman and Thorne, 1988; Thorne, 1990; Allen et al., 1999). Research has shown that increases in the silt-clay content of soils increases their resistance to entrainment (Thorne and Tovey, 1981; Osman and Thorne, 1988). In contrast, soils with high silt-clay contents are more susceptible to the effects of SAP, which make the soils less resistant to erosion by hydraulic forces (Couper, 2003).

Roberts et al. (1998) conducted flume studies to determine the effects of bulk density and particle size on the erosion of quartz particles. Mean particle sizes ranged from 0.005-1.35 mm and the particle size distributions were small. Bulk densities were 1.65-1.95 g/cm^3, while shear stress was varied from 0.2 Pa to 6.4 Pa. The authors defined the critical shear stress (τ_c) as that shear stress which produced an erosion rate of 10^{-4} cm/s. The results indicated that, for particles less than 0.222 mm in diameter, erosion rate decreases rapidly with increasing bulk density. For larger particles, the erosion rate is independent of the bulk density. For a given bulk density, erosion rate increases with increasing particle size, reaches a maximum, and then decreases with further increases in particle size. Correspondingly, the τ_c decreases with increasing particle size, reaches a minimum for particle sizes on the order of 0.02 mm, and then increases with increases in particle size. The authors noted that at very small particle sizes, erosion occurred as aggregates, despite the fact that the particles were quartz.

Since cohesive soils are often eroded as entire aggregates, aggregate size distribution and aggregate stability play an important role in the erosion of cohesive soils. Aggregate breakdown creates smaller particles which are more susceptible to erosion. Aggregate stability is most influenced by soil texture, clay mineralogy, organic matter content, type and concentration of cations, and soil sesquioxide and $CaCO_3$ content.

Loss of aggregate stability is the result of slaking, differential swelling, raindrop impact and physico-chemical dispersion (Le Bissonnais, 1996). Slaking is the breakdown of soil aggregates from the compression of entrapped air during rapid soil wetting. Slaking decreases with increasing soil moisture, due to a reduced volume of air in the soil and a reduction in matric potential gradient. Slaking is also reduced for soils with clay contents in the range of 100-300 g/kg. Haynes and Beare (1997) determined decreases in aggregate stability were positively correlated with soil moisture content and attributed this finding to the effects of soil slaking.

Both internal and external forces reduce aggregate stability. Differential swelling and shrinking occur during the wetting or drying of clay soils, creating internal stresses due to nonuniform volume changes. These nonuniform changes in soil volume increase with increasing clay content. Raindrop impact, an external force, physically breaks aggregates apart.

Physico-chemical dispersion is caused by the decrease in attractive forces between clay particles during wetting. The clay fraction in soils consists of silica tetrahedra (T) and alumina octahedra (O) sheets in platelets with configurations of OT or TOT (Paaswell, 1973; McBride, 1994). Due to isomorphic substitution within the crystals, clay platelets typically exhibit a surface charge. The magnitude of the charge depends on the valence difference between the original and substituted cation and the location of the charge in the crystal lattice. Because a negative charge typically exists on the surface of clay platelets, cations are held in the region between the clay layers. Associated with these cations are water molecules which move freely in and out of the interlayer region. This interlayer water can be removed by soil drying or freezing. Alternatively, exposing the clays to a high electrolyte solution can drive the water out of the interlayer region due to osmotic differences. Removal of this interlayer water reduces the interlayer spacing and increases soil stability. Conversely, if the electrolyte concentration of the surrounding solution is reduced, water will migrate into the interlayer region and increase spacing between the silicate sheets. The degree of shrinking and swelling that occurs depends on the size and valence of the interlayer cations, as well as the type of clay (Martin, 1962). While all clays expand due to hydration of the interlayer cations, osmotic swelling typically occurs only for soils with monovalent cations in the interlayer region. Multivalent cations, such as Ca^{2+} and Mg^{2+} have smaller hydrated radii than monovalent cations and reduce soil swelling by forming "electrostatic bridges" between clay platelets (McBride, 1994).

Among the 2:1 (TOT) clays, montmorillonites have greater swelling potential than illites because the small potassium molecules in the interlayers of illite strongly bond the clay layers together. Clays with pH dependent surface charge, such as kaolinites or illites, are more dispersible at higher pH due to increases in the soil cation exchange capacity (and, therefore, the number of interlayer cations) with increasing pH. Increases in pore water content decrease the interparticle forces in soil, leaving soil vulnerable to entrainment (Craig, 1992). The diffuse double layer theory of soils proposes that the inverse of the distance over which the soil surface charge extends ($1/\kappa$) is determined as follows:

$$\kappa = A \cdot z \cdot \left(\frac{n_o}{\varepsilon \cdot k \cdot T} \right)^{0.5} \qquad 2.1$$

where A is a constant, z is the cation charge, n_o is the cation concentration, ε is the dielectric constant of the eroding fluid, k is the Boltzmann constant, and T is the temperature. In general, the double layer thickness increases as the pore water cation concentration and valence decrease and temperature increases. Increases in the double-layer thickness result in increased repulsion between soil particles and increased interlayer spacing. Dispersion is highly effective at breaking down aggregates and also increases the effectiveness of the other aggregate breakdown methods.

2.2.2. The Effects of Subaerial Processes on Fluvial Entrainment

It is well recognized that the resistance of stream bank soils to fluvial entrainment changes over time as soil moisture and temperature fluctuate. Several researchers have observed that bank erosion is greatest during the winter and have attributed this to freezing of stream banks (Wolman, 1959; Lawler, 1986; Stott, 1997). Freezing of the stream bank surface causes a migration of soil water to the bank surface, increasing the local moisture content. Also, as the soil water freezes and expands, it increases the soil volume (Lawler, 1993). This increase in moisture content and decrease in density due to FTC makes soils more susceptible to fluvial entrainment.

Lawler (1986) measured stream bank retreat due to the combined effects of subaerial processes and fluvial entrainment for two years along two meander bends in South Wales. The watershed area was 30 km^2 and the bank soils were 21-83% silt-clay. A network of 208 erosion pins were measured monthly to determine bank retreat rates. The author noted that bank retreat was most severe in the winter: frost action loosened the soil on the surface of the stream banks, producing a friable, easily eroded layer. Comparing the measured retreat rates to meteorological conditions using multivariate and bivariate analyses, Lawler found the incidence of frost produced the best prediction of average and maximum bank retreat and that air frost and rainfall frequency were most significant weather parameters for bank retreat predictions.

In a study of needle ice formation, Lawler (1993) monitored stream bank retreat rates along an unvegetated meander bend in the River Ilston, West Glamorgan, UK for 2.25 years. Data from erosion pins were related to river discharge and air, stream, and soil temperatures. The occurrence of needle ice was responsible for 32% and 43% of the annual stream bank retreat recorded during the study. Total bank movement over the study period was 0.145 m, with most of the retreat occurring between November and April of each year. It was estimated that an average of 18.8 needle ice events occurred, which is typical of humid temperate environments (Lawler, 1988). Lawler also noted that, in addition to delivering soil directly to the stream, needle ice formation created a friable, “puffy” layer of soil on the bank surface that was easily eroded by subsequent flows. Significant bank retreat was observed when high stream stages were preceded by FTC. The author theorized that if this loosened soil was not removed by high flows following the FTC, soil strength would increase over time due to reconsolidation (Lawler, 1993).

Robinson et al. (2000) measured the effects of surface weathering processes on gully erosion rates. A large outdoor flume (1.8 m wide, 29.3 m long, 2.4 m high) was filled with a red sandy clay soil and an overfall was created. Eight flow events were conducted between July 1999 and May 2000. Submerged jet testing was conducted before and after each run and the soil surface was surveyed periodically. Between each run, the flume was left exposed. The researchers observed cracking of the soil surface and the creation of distinct peds as a result of weathering. Weathering also created a surface crust due to rainfall and/or FTC. This weathered surface extended to a depth of 35-45 cm and resulted in initially high erosion rates for runs following weathering events. This observation was supported by jet test measurements which showed a 160-fold increase in the erodibility coefficient as a result of surface weathering.

Gatto and Ferrick (2002) conducted laboratory studies of rill development following FTC. Bins of compacted soil (79 cm long, 37 cm wide, 18 cm deep) were frozen and eroded at two different flow rates. Soil moisture content and slope were varied among the bins and the total mass of soil eroded was compared between the frozen bins and unfrozen controls. Differences in soil erosion between the unfrozen and frozen soils increased with increasing moisture content: soil loss from the high moisture content samples (MC of 36-38%) was as much as 6.2 times that of the corresponding controls. The authors concluded that FTC increases soil erodibility, but the effect "varies with soil texture, moisture, and extent of freezing."

Currently, there is a lack of published data on in situ changes in stream bank temperature and moisture content over long periods and the effects of SAP on soil critical shear stress and soil erodibility have yet to be quantified (Lawler et al., 1997).

2.2.3. Modeling Fluvial Entrainment

Fluvial entrainment is the result of shear stress on the stream bed and banks. The boundary shear stress is proportional to the velocity gradient near the channel bed or banks. The shear stress on the channel bed is typically defined by the following relationship:

$$\tau_f = \gamma RS \qquad 2.2$$

where τ_f is the average total fluvial shear stress on the channel bed (Pa); γ is the unit weight of water (N/m^3); R is the channel hydraulic radius (m); and S is the energy slope (m/m). Shear stress on the banks will be less than that on the bed, depending on channel dimensions (Chow, 1959). Thorne et al. (1997) noted that while some sediment movement can occur even at low shear stresses, significant soil loss typically does not occur until the boundary shear stress exceeds a critical value (τ_c). Traditional methods of assessing τ_c for noncohesive soils use a Shields-type entrainment function (Langendoen, 2000). The Shields diagram (Figure 2.2) indicates the shear stress to initiate motion, given flow and particle properties.

For cohesive soils, critical shear stress is difficult to predict accurately; there is no precise definition of critical shear stress and there are discrepancies among researchers (Heinzen, 1976; ASCE, 1998a). Two general approaches to determine τ_c have been used (Hollick, 1976). In the first approach, soil samples are exposed to a hydraulic stress and the shear stress at which erosion starts is noted. The problem with this approach is defining the point at which erosion starts. Dunn (1959) conducted laboratory submerged jet tests and defined τ_c as the shear stress that caused enough erosion to make the water continuously cloudy. Smerdon and Beasley (1961) conducted erosion studies of cohesive soils in a 60-foot flume. They defined τ_c as the shear stress that caused "general movement" of the bed material.

The second method measures the erosion rate of the samples at various shear stresses; the erosion rate is then plotted versus shear stress and a straight line is fitted to the data. The shear stress at which the line crosses the x-axis (zero erosion rate) is then used as the critical shear

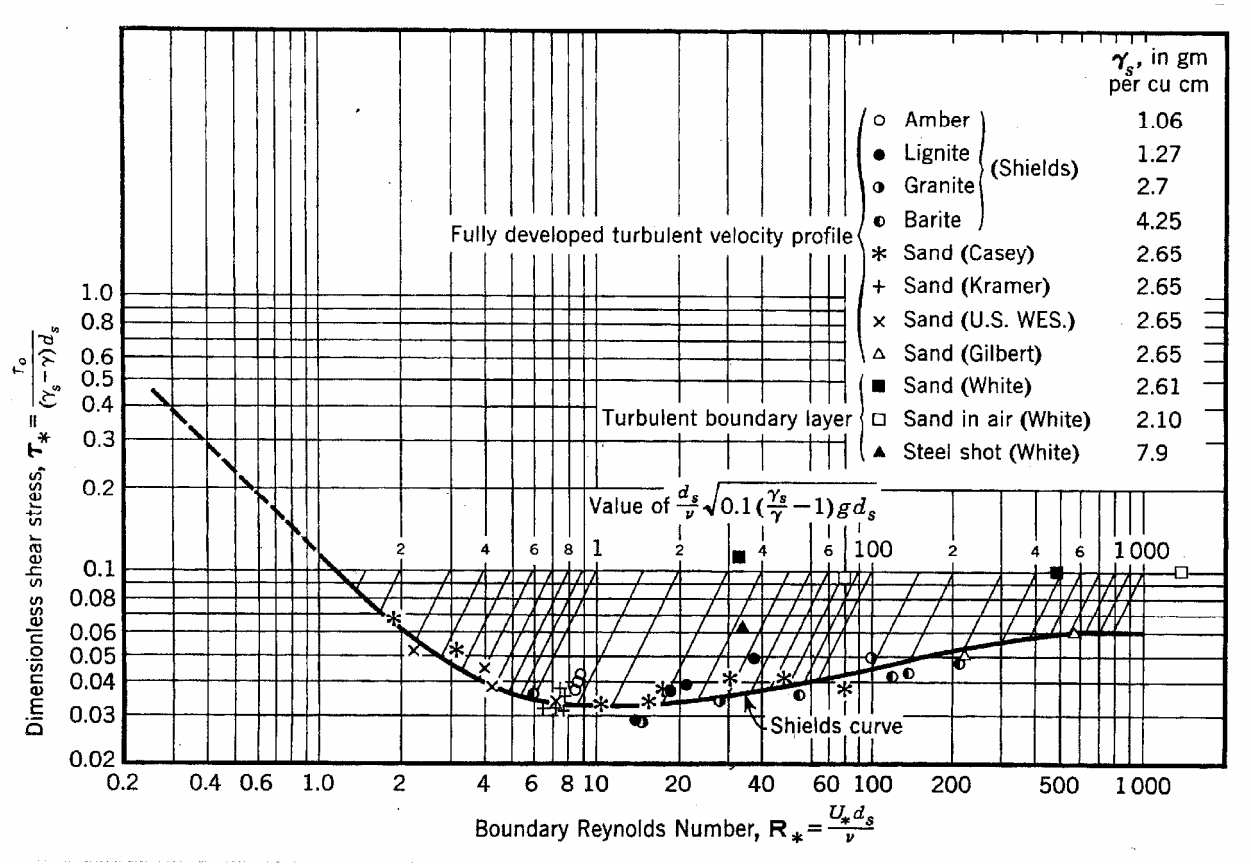

Figure 2.2. Shields diagram (reprinted with permission of ASCE from Sedimentation Engineering, V. A. Vanoni, ed. 1975. ASCE: New York).

stress (Hanson and Cook, 1997). Some researchers have suggested that a critical shear stress, such as that observed with noncohesive soils, does not exist for cohesive soils (Anderson, 1975; Lavelle and Mofjeld, 1987).

In general, the critical shear stress for cohesive soils is greater than that for noncohesive soils, but it varies widely. In 1975, an ASCE task committee observed that reported critical shear stresses for cohesive soils varied as much as 200-fold (Anderson, 1975). Several researchers have developed empirical relationships between the critical shear stress of cohesive soils and soil properties, but the prediction of fluvial entrainment rates based on soil physical properties has had limited success (Dunn, 1959; Smerdon and Beasley, 1961; Carlson and Enger, 1963; Lyle and Smerdon, 1965; Alizadeh, 1974).

Dunn (1959) determined the τ_c for remolded samples taken from streams in the western US. Soil textures ranged from sand to silty clay and at least two different consolidation

pressures were used to mold each sample. The τ_c was determined using a submerged jet impinging normally on the sample. Hydraulic shear stress was measured by placing a 1 in^2 plate at the location of the greatest soil scour. The following relationship was determined for soils with a plasticity index of 5-16:

$$\tau_c = 0.001 \cdot (S_v + 180) \cdot \tan(30 + 1.73 \cdot PI) \qquad 2.3$$

where τ_c and the shear strength of the soil (S_v) are in psi, PI is the plasticity index in percent and the argument of the tangent is in degrees. A rotating vane was used to determine S_v. Significant correlation between τ_c and the silt+clay content of the soils was determined for those soils with a high sand content. Increasing the fraction of fine particles in these coarser soils from 12.5% to 26% increased τ_c an order of magnitude.

Smerdon and Beasley (1961) tested 11 Missouri soils to determine the relationship between τ_c and soil properties. The soil was loosely compacted in a flume and the hydraulic shear stress was increased in increments until "general movement" of the bed was observed. This point was defined as the critical tractive force. Soil properties, including Atterberg limits, void ratio, aggregate analysis, specific gravity, particle size analysis and dispersion ratio, were measured and compared to τ_c values using regression analysis. Significant simple linear regression relationships were found between τ_c and the soil plasticity index (PI), dispersion ratio (D_r), median grain size (D_{50}), and percent clay. The critical tractive force increased with increasing PI and percent clay, and decreasing D_r and D_{50}.

Alizadeh (1974) developed a chart to predict the critical shear stress as a function of the soil sodium adsorption ratio (SAR), the dielectric dispersion, and the pore water salt concentration (TS), using artificial soil mixtures with distilled water as the eroding fluid (Figure 2.3). The SAR is defined as follows:

$$SAR = \frac{\left[Na^{+}\right]}{\sqrt{\left(\frac{\left[Ca^{2+}\right]+\left[Mg^{2+}\right]}{2}\right)}} \qquad 2.4$$

where $[Ca^{2+}]$, $[Mg^{2+}]$ and $[Na^{+}]$ are the concentrations (meq/L) of calcium, and magnesium, and sodium, respectively, in the soil pore water. This analysis does not consider the effects of soil structure and aggregate stability on soil erosion (Thorne, 1982). Also, because distilled water was used as the eroding fluid, these values represent the lower bound of critical shear stress for soils.

Arulanandan et al. (1975) studied the effects of pore and eroding fluid on the erosion of a Yolo Loam. The TS and SAR, as well as the eroding water salt concentration were varied. The soil τ_c was determined using a rotating cylindrical apparatus, which consisted of two concentric cylinders with 0.5 in annular space between. Soil samples were sieved and remolded into 7.6 cm diameter, 8.1 cm long cylinders. The space between the soil sample and the outer cylinder was filled with fluid and the outer cylinder was rotated to produce hydraulic shear on the sample. The researchers determined the erosion rate increased with increasing SAR of the pore fluid, while τ_c decreased (SAR of 1.4-154). Additionally, decreases in τ_c with increasing SAR were more pronounced at low SAR; at higher SAR, τ_c changed little with increases in SAR. Increases in TS resulted in increased τ_c, likely due to increased soil flocculation at high salt concentrations (TS of 0.1, 0.01, and 0.005 *N*). The authors also evaluated the effects of SAR on the swelling of soils at a TS of 0.005 *N*. Soil swelling increased with increases in SAR. Soil swelling has significance for erosion because swelling increases the distance between soil layers and reduces interparticle bonding, effectively reducing τ_c. Lastly, the effect of salt concentration in the eroding fluid was investigated. The erosion rate increased and τ_c decreased with decreasing NaCl concentrations in the eroding fluid, while little erosion occurred at NaCl concentrations over 0.02 *N*. The increased erosion with decreasing eroding fluid salt concentration was attributed to osmotic differences between the soil pore water and the eroding fluid. When the salt concentration of the pore fluid is higher than that of the eroding fluid, water will move into the soil, cause the soil to swell, and weaken interparticle forces. The magnitude of this depends on how susceptible the soil is to swelling. When the electrolyte concentration of the eroding

fluid is greater than that of the pore water, water migrates out of the interlayer region and the soil structure collapses, increasing soil stability.

Heinzen (1976) measured the soil erodibility and critical shear stress of 11 undisturbed soil samples in a small flume, using distilled water as eroding fluid. Several methods of predicting soil erodibility were compared. The TS, dielectric dispersion, SAR, organic matter content, cation exchange capacity (CEC), Atterberg limits, dispersion ratio, texture, and density of the test soils were measured. Free swell tests were also conducted. Heinzen noted that the overall structure of the undisturbed samples played a significant role in their behavior during erosion. The results indicated that erodibility methods that consider the chemical interaction between the pore water and eroding fluid provide the best prediction of soil erodibility.

Arulanandan et al. (1980) conducted flume studies using undisturbed soil and stream water samples from across the U.S. with the goal of developing a quantitative method to predict the τ_c and the erosion rate of undisturbed natural soils. The results indicated that τ_c decreased with increasing soil pore water SAR. Additionally, as the salt concentration of the eroding fluid increased, the soil became more resistant to erosion. Figure 2.3 was developed to predict τ_c, given the soil pore water SAR, the soil dielectric dispersion, and the salt concentration of the eroding fluid. Once τ_c is known, the erosion rate can be estimated from Figure 2.4, which shows the rate of change in the erosion rate at a given τ_c.

Osman and Thorne (1988) developed a model of bank toe erosion, based on the work of Arulanandan et al. (1980). The critical shear stress for the bank material is determined from Figure 2.3. If the stream shear stress is greater than τ_c, an initial rate of bank erosion (E_i) is determined as:

$$E_i = \frac{0.0223}{\gamma} \tau_c e^{(-0.13\tau_c)} \qquad 2.5$$

The actual soil erosion rate (E) is assumed to vary linearly with excess shear stress and is given by the following:

$$E = E_i\left(\frac{\tau_f}{\tau_c} - 1\right) \qquad 2.6$$

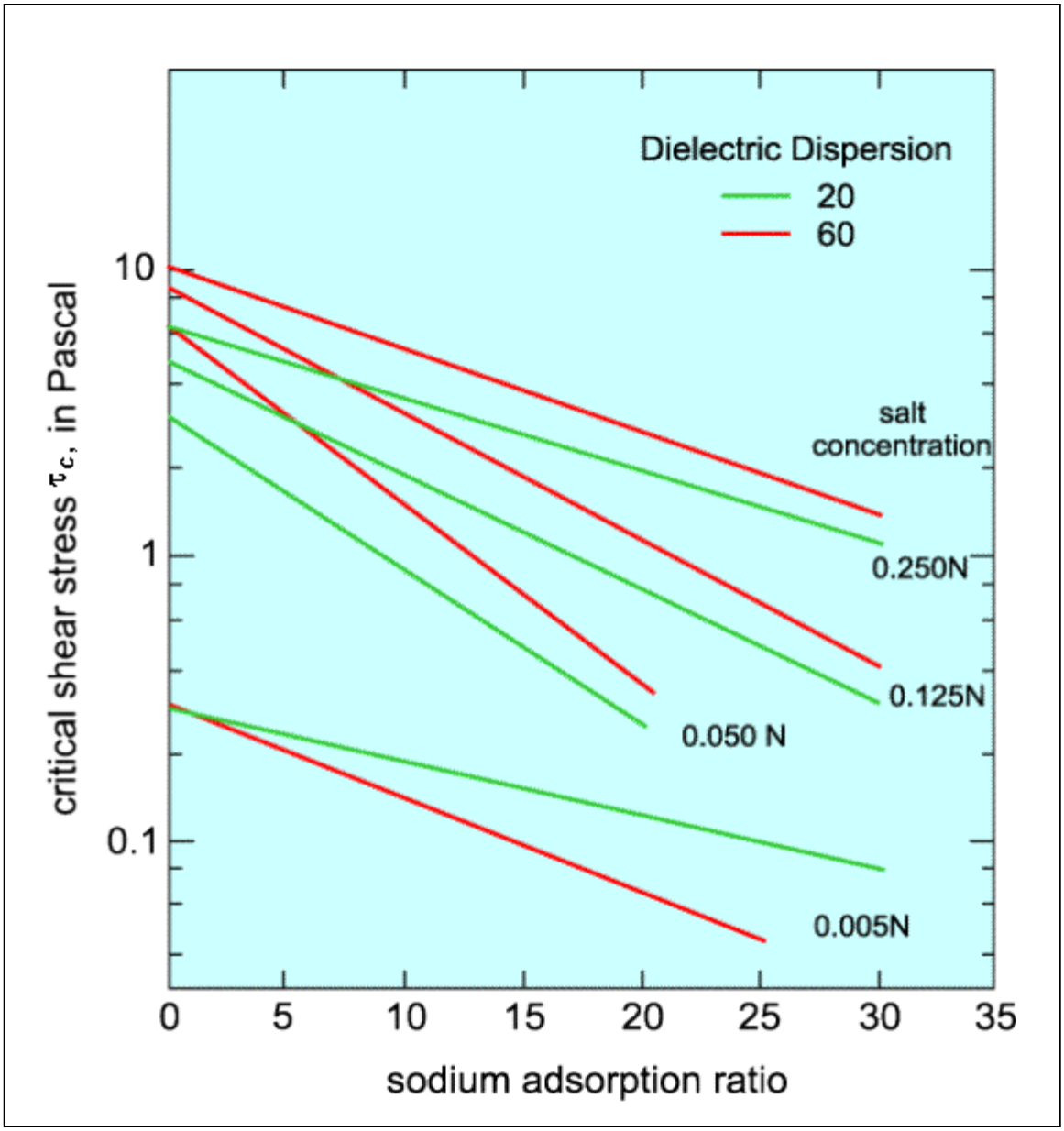

Figure 2.3. Critical shear stress versus sodium adsorption ratio for different salt concentrations (*N*) and dielectric dispersion values (modified from Langendoen, 2000, as modified from Arulanandan et al., 1980).

Here, the rate of fluvial erosion is modeled as a function of the difference between the actual boundary shear stress and the critical shear stress. The erosion rate increases linearly once the shear stress exceeds the critical value (Langendoen, 2000).

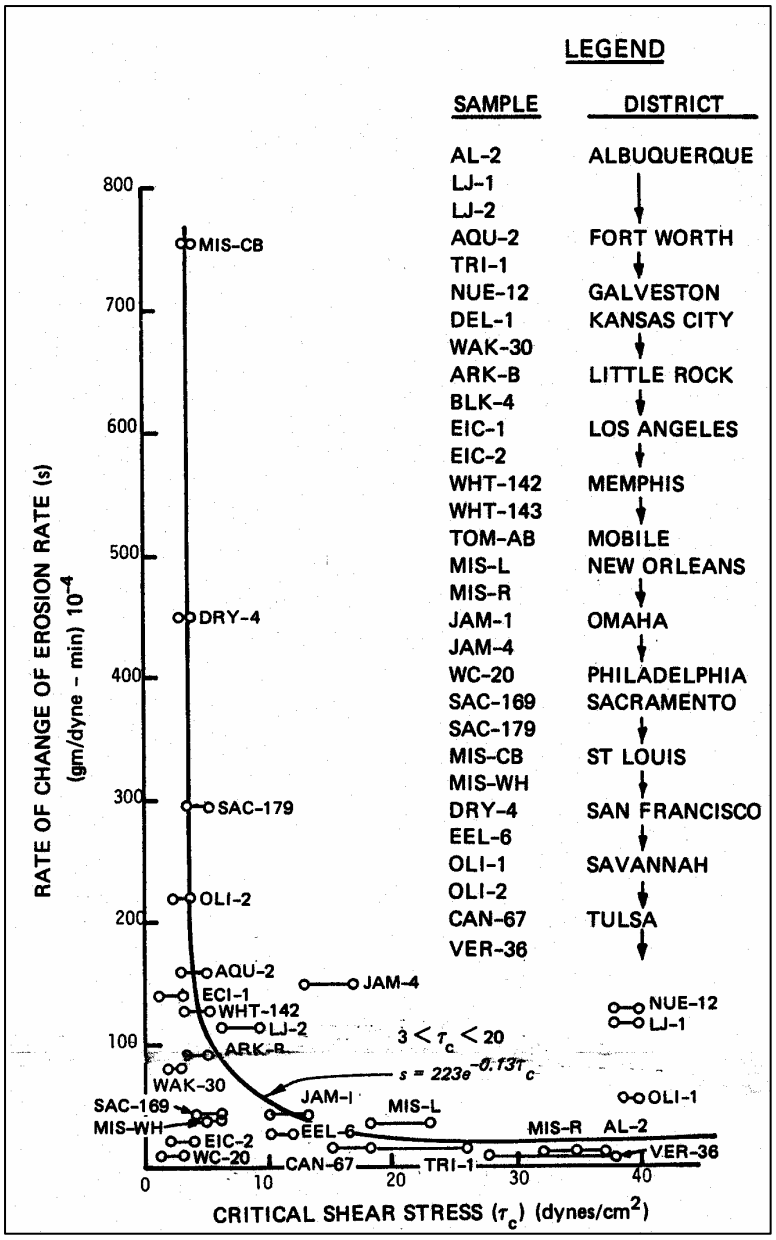

Figure 2.4. The rate of change of erosion rate versus the critical shear stress for undisturbed cohesive soils using distilled water as the eroding fluid (Arulanandan et al., 1980).

A similar, commonly used expression for the rate of soil erosion is the excess stress equation:

$$E = K_d(\tau_f - \tau_c)^b \qquad 2.7$$

where E is the erosion rate ($cm^3/hr/cm^2$); K_d is the erodibility coefficient (cm/hr/Pa); τ is the actual shear stress (Pa); τ_c is the critical shear stress (Pa); and b is an exponent that is often assumed to equal one (Hanson et al., 1999). Combining equations 2.5 and 2.6 and comparing them to equation 2.7, it can be seen that K_d equals E_i/τ_c. The erosion resistance of the soil is incorporated in both of the parameters, K_d and τ_c (Owoputi and Stolte, 1995). The excess stress equation is used in several watershed models to calculate sediment erosion by fluvial entrainment, including HEC-6, SWAT, and HSPF (USACE, 1993; Allen et al, 1997; Bicknell et al., 1997). The excess stress equation is also used to model rill erosion in watershed models such as WEPP. Research on rill erosion has shown b can vary between 1.0 and 1.5 (Van Klaveren and McCool, 1998).

The erodibility coefficient can be considered a soil property that can be used to compare relative erodibility and to classify soils for design purposes (Heinzen, 1976; Hanson, 1990a; ASTM, 1999a). Various devices have been used to evaluate K_d in laboratory and field studies, including pin hole erosion devices, straight and circular flumes, and rotating cylinders, disks and impellers (Allen et al., 1997). Several researchers have used an impinging jet to study scour because the initial flow pattern can be described by the jet size and velocity and that a characteristic depth can be used to describe the scour (Rouse, 1940; Laursen, 1952; Dunn, 1959). Laursen (1952) proposed that the rate of scour beneath a jet will decrease with time as the sour hole enlarges and will asymptotically approach zero as the decreasing hydraulic force approaches the resistance of the soil.

Hanson (1989; 1990a; 1990b; 1991) developed an *in situ* testing procedure to determine K_d and τ_c of channel beds using a submerged, vertical jet device. Several studies have used submerged jets for determining soil critical shear stress (Dunn, 1959; Moore and Masch, 1962; Hollick, 1976). A similar device for testing bank material has been developed in cooperation with the USDA Sedimentation Laboratory in Oxford, MS (Hanson, 2001). Hanson and Cook (1997) adapted analytical procedures developed by Stein et al. (1993) and Stein and Nett (1997) for a planar overfall jet to determine K_d and τ_c for scour created by a submerged jet. Figure 2.5 shows a diagram of the submerged jet testing device. A circular jet at a uniform velocity, U_o, is produced by a nozzle of diameter d_o, under pressure h, and hits the soil bed at right angles. The jet velocity is calculated as follows:

$$U_o = C\sqrt{2gh} \tag{2.8}$$

where *g* is the acceleration due to gravity, h is the head on the jet, and C is a nozzle coefficient that can be assumed to be one, since the nozzle is round. The velocity of the jet remains constant at U_o over a core length of H_p. Beyond H_p, the velocity is reduced by diffusion, although it maintains a maximum velocity along the jet centerline. Initially, the jet is at a height, H_i, above the soil. The jet scours the soil until the maximum scour depth is reached at H_e. Assuming the rate of change in scour depth, dH/dt, is the erosion rate, as a function of the maximum boundary stress, and H_i is greater than H_p, then the erosion rate can be expressed as follows:

$$\frac{dH}{dt} = K\left(\frac{\tau_o H_p^2}{H^2} - \tau_c\right) \tag{2.9}$$

where τ_o is the maximum applied bed shear stress within the jet core and t is the time of scour.

When the rate of scour equals zero (at H_e), the critical shear stress can be computed as follows:

$$\tau_c = \tau_o\left(\frac{H_p}{H_e}\right)^2 \tag{2.10}$$

where

$$H_p = C_d d_o \tag{2.11}$$

and where C_d is a diffusion constant that is typically assumed to have an average value of 6.2 and d_o is the nozzle diameter. Unfortunately, reaching H_e can take anywhere from hours to days (Hanson and Cook, 1997). Due to this limitation, H_e is estimated using a hyperbolic logarithmic method described by Blaisdell et al. (1981). This method assumes the relationship of scour over time follows the logarithmic hyperbolic function (Hanson and Cook; 1997):

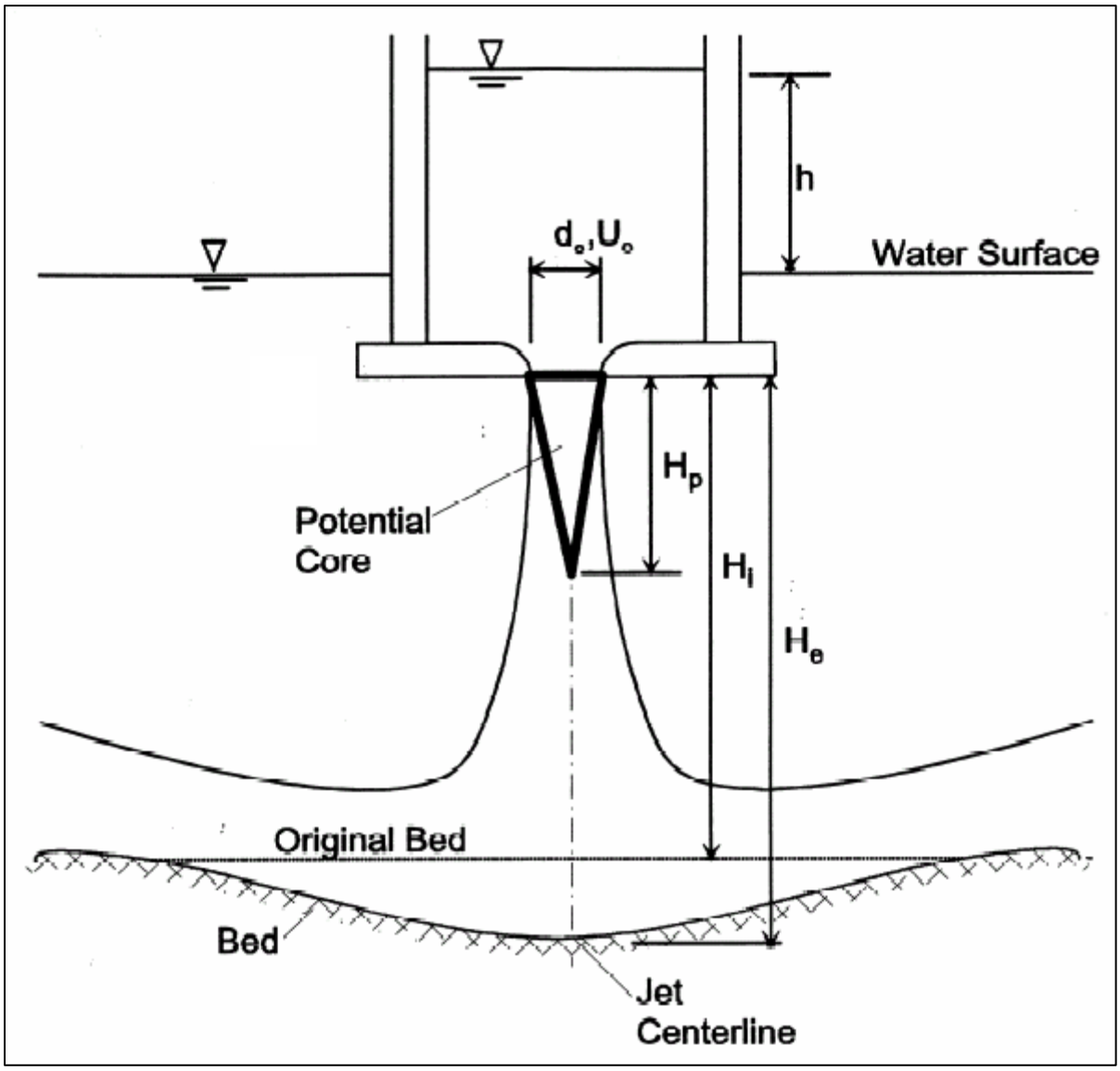

Figure 2.5. Schematic of submerged jet testing device (Hanson and Cook, 1997). Used with permission from the American Society of Agricultural Engineers.

$$x = \left[(f - f_o)^2 - A^2 \right]^{0.5} \quad \text{where} \tag{2.12}$$

$$x = \log\left(\frac{U_o \cdot t}{d_o} \right) \quad \text{and} \tag{2.13}$$

$$f = \log\left(\frac{H}{d_o}\right) - \log\left(\frac{U_o \cdot t}{d_o}\right) \quad \text{and} \tag{2.14}$$

$$f_o = \log\left(\frac{H_e}{d_o}\right) \tag{2.15}$$

where f_o is the asymptotic value of the hyperbola, *A* is the value of the semi transverse and semi conjugate axis of the hyperbola, t is the time, and H is the depth of scour at time, t. An iterative procedure is used to find f_o and *A* by minimizing the standard error. The values for H_e and τ_c can then be calculated.

Using Equation 2.10, Equation 2.9 can be written in the following dimensionless form:

$$\frac{dH^*}{dT^*} = \frac{\left(1 - H^{*2}\right)}{H^{*2}} \tag{2.16}$$

where $H^* = H/H_e$, $H_p^* = H_p/H_e$, $T^* = t/T_r$, and $T_r = H_e/(K_d \tau_c)$. Integrating Equation 2.16 from the nozzle to the depth of scour results in the following dimensionless relationship:

$$T^* = 0.5\ln\left(\frac{1+H^*}{1-H^*}\right) - H^* - 0.5\ln\left(\frac{1+H_p^*}{1-H_p^*}\right) + H_p^* + \frac{H_p^{*3}}{1-H_p^{*2}} \tag{2.17}$$

Equation 2.17 can be reduced to a more useful form for analysis:

$$t_m = \frac{H_e^3}{K\tau_o H_p^2}\left[0.5\ln\left(\frac{1+H^*}{1-H^*}\right) - H^* - 0.5\ln\left(\frac{1+H_i^*}{1-H_i^*}\right) + H_i^*\right] \tag{2.18}$$

where t_m is the measured time from the start of the jet test. The two unknowns, H_e and K_d, need to be fitted, such that the predicted t_m most closely matches the actual t_m. The estimate of H_e is used to narrow the possible combinations of H_e and K_d, and a least-squares regression of the predicted t_m versus the actual t_m is used to obtain the best fit estimates of H_e and K_d. The critical shear stress is computed from Equation 2.10. These analytical procedures have been coded in an Excel spreadsheet by Hanson and Cook, as modified by the author for data input in SI units. Figure 2.6 shows a plot of H* versus T* with the best fit line from site ST2.

Allen et al. (1997) used Hanson's jet test device to develop predictive equations of soil erodibility in Texas for use in the SWAT model. They used data from 30 streams and stratified the soils based on the percentage of clay and the soil activity. Soils were tested for bulk density, void ratio, Atterberg limits, and soil texture. A highly significant regression was obtained for each of the three soil categories (r^2 = 0.78-0.96). For soils with less than 10% clay, the antecedent moisture content and the percentage of sand were the most important predictors of soil erodibility. The second category contained soils with >10% clay and activities <1.25. Bulk density, percent clay, and plastic limits were the best indicators of erodibility for these soils. The most cohesive soils were in the third category, where clay contents and soil activities were higher than 10% and 1.25, respectively. For these soils, the complete soil textural classification and the liquid limit produced the best prediction of soil erosion potential. Additionally, the authors noted that the presence and density of roots seemed to influence soil erodibility, although this parameter was not quantified. The authors demonstrated an application of the data in a SWAT model to evaluate the effects of urbanization and climate change on long term channel degradation.

2.3. Mass Wasting

Mass wasting occurs when the weight of the bank is greater than the shear strength of the soil (Osman and Thorne, 1988). It often results from increases in bank height or bank angle due to fluvial erosion and the presence of tension cracks (ASCE, 1998a; Simon et al., 2000). Mass wasting depends on bank geometry and stratigraphy, properties of the bank materials, and the type and density of bank vegetation (Thorne, 1990; Abernethy and Rutherfurd, 1998).

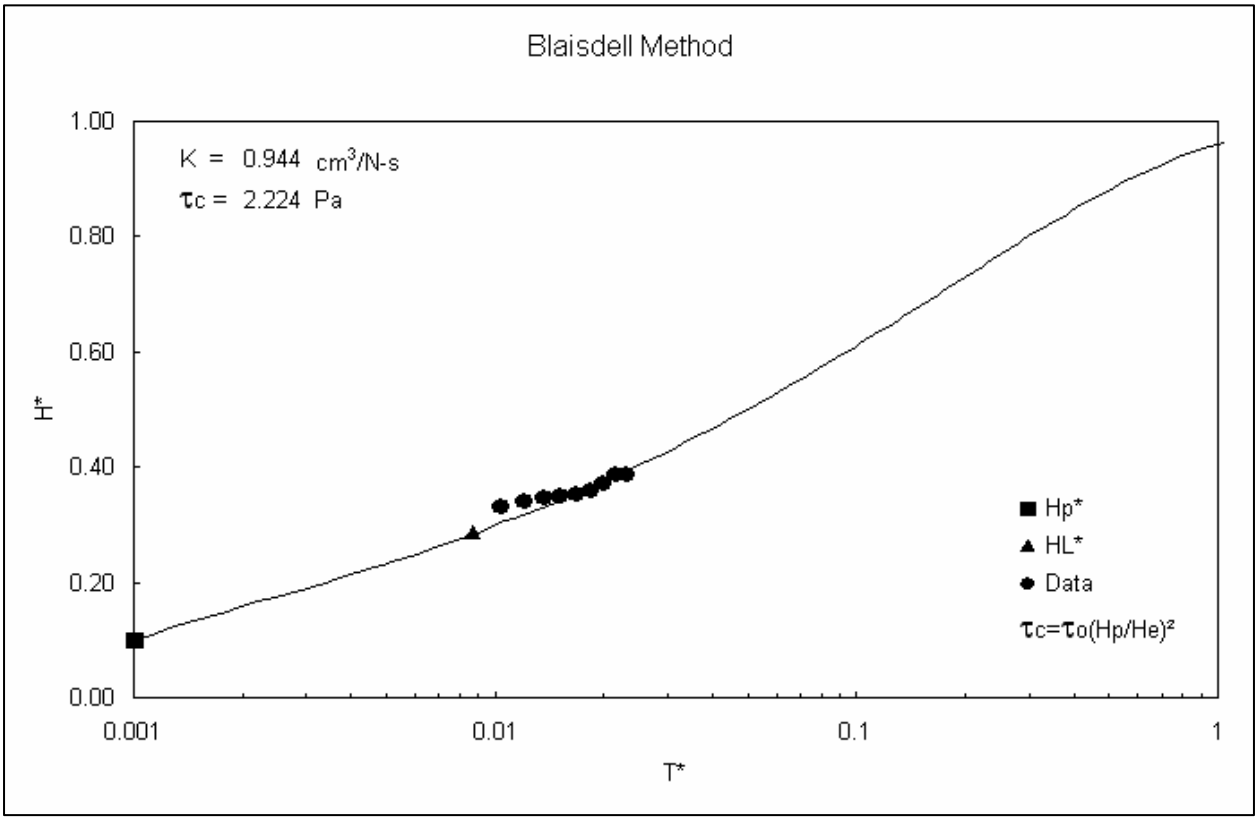

Figure 2.6. Plot of H* versus T* with best fit regression line for site ST2, test 1, upper bank.

Mass failures often occur following floods. Precipitation and a rising stream stage increase the moisture content and weight of bank soils. At the same time, apparent soil cohesion is decreased through the reduction of matric suction. If rainfall is prolonged, positive pore pressures may develop, resulting in a decrease in frictional soil strength. Additionally, the bank height or angle may be increased as flood waters scour the channel bed or bank toe (basal area). These changes, combined with a rapid loss of confining pressure as the stream stage recedes, can trigger mass failures (Figure 2.7).

2.4. Process Dominance

While it is difficult to determine which process(es) is(are) the cause of bank retreat in any specific case, it has been observed that the driving forces vary with location in a fluvial system (Lawler, 1992; Lawler, 1995; Abernethy and Rutherfurd, 1998; Lawler et al., 1999). In the upper reaches of a watershed, stream slope and elevation are high, while stream discharge and

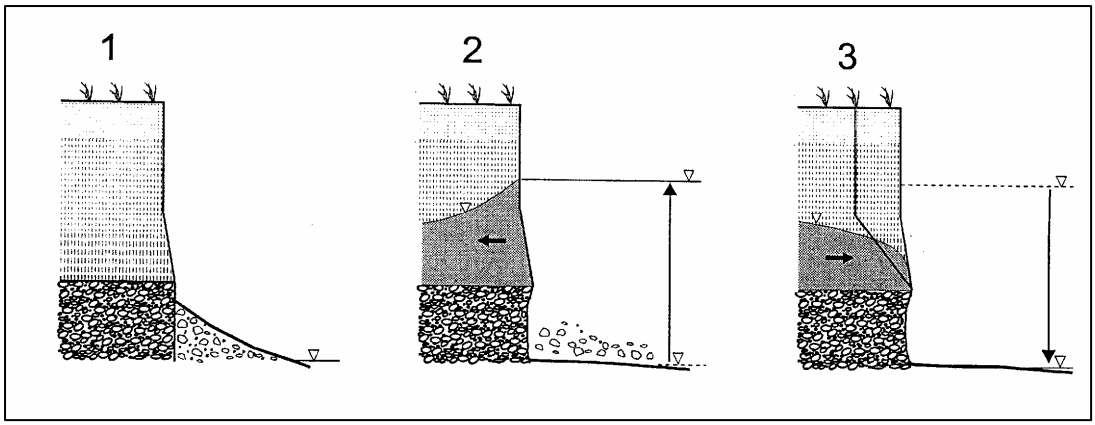

Figure 2.7. Bank failure where basal sediment (1) is removed by high flows (2) which increases the bank angle and saturates the bank (3), leaving the stream bank prone to mass failure (Reprinted from *Geomorphology*, 26(4), M. Rinaldi and N. Casagli, Stability of streambanks formed in partially saturated soils and effects of negative pore water pressures: the Sieve River (Italy), 253-277, 1999, with permission from Elsevier.)

bank height are small. Stream sediments are typically dominated by coarse materials. Because of this combination of factors, fluvial entrainment and mass wasting are generally secondary to SAP, such as FTC. Although SAP act throughout a watershed, they are most noticeable in headwater areas (drainage areas < 85 km^2) where temperatures are colder and the other stream bank retreat processes are reduced. With increasing distance downstream, channel slope and sediment size decrease, while stream discharge and bank height increase. These effects combine to peak fluvial entrainment in the middle reaches. In the lower reaches of a river system, bank heights increase further and mass wasting becomes dominant. Although discharge is greatest in the lower reaches of a river system, the channel sediments are typically dominated by erosion-resistant clays and the stream slope is low; thus, fluvial entrainment is of secondary importance. Because these areas are at a lower elevation, air temperatures are higher than in the headwaters and desiccation takes on greater importance than FTC.

2.5. Basal Endpoint Control

While the above described model of process dominance has been supported by research (Abernethy and Rutherfurd, 1998; Lawler et al., 1999), bank erosion processes often work in concert and the significance of each process is a function of the properties of the individual bank

system (Grissinger, 1982). Bank erosion mechanisms are linked in a process termed *basal endpoint control* where the balance between the rate of bank material delivery to the basal area and the subsequent removal rate of that material by the stream determine the ultimate rate of bank retreat (Thorne, 1990). Initially, fluvial erosion removes material from the stream basal area, increasing bank height and/or angle. This removal causes mass instability and failure of the bank. The failed material is delivered to the toe of the bank; it may be immediately entrained or it may remain at the toe until subsequent high flows remove it. If the material is not removed, it will reinforce the bank and reduce further mass failures. Three states of basal endpoint control are defined as follows (Thorne, 1982):

1. Impeded removal - The supply of failed material exceeds the ability of the stream to remove it. The failed material serves to stabilize the bank, reducing the supply of eroded soil.
2. Unimpeded removal - The supply and removal rates are equal, such that the bank height and angle remain constant. The rate of parallel bank retreat is controlled by the stream flow.
3. Excess basal capacity - The material removal rate exceeds the supply from the banks. This high removal rate leads to scour of the basal area, increasing the bank height and angle and decreasing bank stability. This instability increases the supply of material to the stream and moves the system toward a state of unimpeded removal.

2.6. Effects of Vegetation on Stream Bank Stability

Little specific information is available on the effects of vegetation on stream bank stability (Abernethy and Rutherfurd, 1998). It is generally established that vegetation influences the chemical and physical properties of stream banks, as well as the local microclimate. The following sections describe the effects of vegetation on the three processes implicated in stream bank retreat. Also, the impacts of woody versus herbaceous plants are compared.

2.6.1. Subaerial Processes

Riparian vegetation has multiple effects on SAP (Wu, 1984; Abernethy and Rutherfurd, 1998). A dense cover of vegetation absorbs the energy of rainfall, reducing soil detachment by raindrop impact (Gray and Leiser, 1982; Coppin and Richards, 1990). Sheet and rill erosion are

decreased several orders of magnitude due to interception storage, improved infiltration, increased flow resistance, and the stabilizing influence of roots on surface soils (Thorne, 1982; Gurnell and Gregory, 1984; Thorne, 1990). Alternatively, roots may increase the susceptibility of a bank to fluvial erosion by loosening the bank soil (Thorne, 1990).

Vegetation insulates the stream bank from extreme temperature fluctuations (Abernethy and Rutherfurd, 1998). This insulation minimizes the occurrence of freezing and cracking due to desiccation (Thorne, 1990). Amarasinghe (1992) found a decrease in evaporation improved soil moisture retention in vegetated banks, as compared to bare banks, reducing the risk of desiccation and slaking. However, Davidson et al. (1991) noted that in dry years, clay stream bank soils under vegetation with high evapotranspiration rates (grass and early successional trees) dried to near the wilting point and developed extensive fissures that lasted for several years. These cracks did not occur under more advanced successional trees which had an extensive litter layer and lower evapotranspiration rates.

The effects of vegetation on winter stream bank soil temperatures were studied in northeastern Nevada (Bohn, 1989). Soil temperature was measured at a depth of 3 cm in four sets of paired bare and vegetated stream banks. Bank vegetation consisted of Kentucky bluegrass and sparse willows. Soil temperatures were recorded every 3 hours from January through May 1987 and average daily soil maximum and minimum temperatures, and daily temperature range were calculated for days when snow cover was absent. Results were analyzed using paired t-tests and showed that the bare stream banks underwent twice the number of FTCs as the vegetated banks. Furthermore, the grass banks had a significantly higher daily minimum temperature and a significantly lower daily maximum temperature, resulting in a lower overall daily temperature range. In addition to reducing near surface wind velocities and insulating against nighttime radiative cooling, vegetation reduces soil bulk densities. The presence of roots and increases in organic matter content result in greater numbers of air-filled pores, which lowers heat conductivity through the soil (Bohn, 1989).

Stott (1997) measured stream bank retreat rates on two streams in central Scotland. One of the streams was dominated by a Sitka spruce plantation, while the riparian area of the second stream contained primarily moorland vegetation, such as grasses, bracken, and heather. Bank retreat rates were measured using erosion pins. Minimum and maximum daily air temperatures

on the stream banks were also recorded on 13 occasions during the six month study period. Bank retreat rates were greatest in the winter on both streams, but the moorland stream had a generally higher retreat rate than the forested stream. The authors attributed this finding to a decreased incidence of frost along the forested stream: air temperatures under the spruce plantation averaged 3.7^{o}C higher than under the moorland vegetation and bank retreat was correlated to the incidence of frost.

2.6.2. Fluvial Entrainment

The influence of vegetation on stream hydraulics has long been recognized (Zimmerman et al., 1967; Hickin, 1984). Vegetation provides increased channel roughness, directing flows towards the center of the channel and reducing flow velocities and shear stresses along the banks (Beschta and Platts, 1986; Gregory and Gurnell, 1988; McKenney et al. 1995; Thorne and Furbish, 1995; Hupp, 1999; Simon and Darby, 1999; Tsujimoto, 1999). Since sediment transport capacity is proportional to flow velocity to the sixth power (v^6), small decreases in stream velocity can result in large changes in sediment transport (Thorne, 1990). Additionally, vegetation damps near bank turbulence and weakens secondary currents in river bends, further reducing fluvial entrainment (Thorne and Furbish, 1995; Abernethy and Rutherfurd, 1998). It should be recognized that the effects of vegetation on stream hydraulics varies with season, stream stage, and stream width to depth ratio, particularly for herbaceous species (Gregory and Gurnell, 1988; Thorne and Osman, 1988; Masterman and Thorne, 1992; Abernethy and Rutherfurd, 2000). Additionally, the spacing of vegetation along a stream is a crucial determinant of the distribution of hydraulic stresses (Pizzuto and Mecklenburg, 1989; Thorne et al., 1997).

Vegetation has multiple effects on the distribution of energy and sediment in a stream. Along streams with forested riparian buffers, fallen trees create series of step pools, dissipating stream energy and providing sediment storage (Beschta and Platts, 1986). Hupp (1999) noted that roots growing under stream channels may provide grade control to limit headcut migration. Additionally, vegetation can act as a nucleus for the creation of sediment bars; vegetation is effective in trapping washload (Hickin, 1984; Thorne, 1990; McKenney et al. 1995; Hupp, 1999). These benefits may be offset by the fact that the presence of downed trees and isolated stands of vegetation can produce locally severe scour of the stream bed and banks, although the

magnitude of this effect depends on the size of the stream or river (Thorne, 1990; McKenney et al. 1995).

2.6.2.1. Effects of Root Density on Soil Erodibility

While considerable research has been conducted on fluvial entrainment, little quantitative information is available on the effects of vegetation on soil scour by concentrated flow (Smith, 1976; Kamyab, 1991; Dunaway et al., 1994; Mamo and Bubenzer, 2001a). It is believed the root systems of woody and herbaceous plants physically bind bank soils in place, increasing τ_c (Gray and Leiser, 1982; Coppin and Richards, 1990; Thorne et al., 1997). Additionally, roots exudates may increase soil cohesion chemically (Amarasinghe, 1992; Thorne et al., 1997). Odgaard (1987) studied erosion along meander bends of two major rivers in Iowa and determined that erosion along wooded stream banks was half that along sparsely vegetated banks.

Smith (1976) measured stream bank erosion rates in Banff Park, Alberta using bank pins and an instream erosion box. These rates were compared to root volume ratios (RVRs, root volume per unit soil volume) under riparian meadow and scrub willow vegetation in silty soils. Root volume ratios ranged from 10% to 21% and the log of the erosion rate decreased linearly with increases in the percentage of root volume. Due to the cold climate, a dense root mat formed on the bank face to depths of 3.5 m and effectively armored the stream bank. This root mat reduced the erosion rate by a factor of 20,000, as compared to bare soil.

Kamyab (1991) measured soil erodibility using soil core samples from three meadow plant communities in the Sierra Nevada Mountains in California. Samples from depth increments of 1-10 cm and 30-40 cm were tested in a laboratory flume under hydraulic stresses of 0.59, 6.2, and 15.7 Pa. The soils were tested for root length density (RLD) and dry root biomass, as well as void ratio, organic carbon, clay content and activity, mean particle size and standard deviation, dispersion ratio, and plasticity index. Root length density is the length of roots in a unit soil volume. Using regression analysis, Kamyab determined erosion resistance was directly proportional to total, fine, and rhizome root length density, as well as total dry root biomass. Erosion was minimal at root length densities in excess of 300 cm/cm^3. At lower RLDs, soil properties, such as clay content, mean grain size, dispersion ratio, and plasticity index influenced soil erosion.

In a follow-up study similar to Kamyab (1991), Dunaway et al. (1994) assessed the interaction between soil and plant characteristics and their impact on erosion rates for riparian meadow communities in the Sierra Nevada Mountains. Samples from the banks of five streams were tested in a flume and the effects of root density, soil texture, and plant community were assessed with multivariate analysis. Average RVR ranged from 0.0027 to 0.0063. Erosion rates were inversely related to RVR and percent silt, but directly proportional to clay content. This is contrary to previous research which showed increasing erosion resistance with increases in clay content (Grissinger et al., 1981). The authors attributed this discrepancy to the low root density of high clay content soils.

Mamo and Bubenzer (2001a) conducted laboratory experiments on the effects of live ryegrass roots on soil detachment, erodibility, and critical shear stress. Soil cores with 100 mm diameters were filled with sieved Plano silt loam and planted at two different densities. The samples were then grown in a greenhouse for periods of six to sixteen weeks. Fallow and rooted soil cores were eroded in a flume using five flow rates of 7.57-37.85 L/min at depths of 3.96-8.23 mm. In addition to measuring erosion rates, soil shear strength, organic matter content, aggregate stability, and root length density were assessed. Results showed that soil strength increased with time for both rooted and fallow soils, but the increase in strength was more significant for the rooted soils. Both soil detachment rate (D_r) and erodibility (K_d) decreased with time and root density. Detachment rates for rooted versus fallow samples decreased 35-73% while erodibility rates were reduced 8-87%. Reductions in both D_r and K_d for both the fallow and planted samples were attributed to increases in interparticle forces with increasing time and successive WDCs. In contrast to soil detachment and erodibility, there were no significant differences in τ_c between rooted and fallow soils and no changes over time were noted. Additionally, there was no apparent relationship between K_d and τ_c, as indicated by previous research (Foster, 1982). The researchers reported an inverse exponential relationship between D_r and root length density, with exponents ranging from -0.02 to -0.50 and correlation coefficients ranging from 0.22 to 0.83. Increases in both aggregate stability and organic carbon content were noted for the rooted samples, while those properties remained constant in the fallow cores.

Mamo and Bubenzer (2001b) extended their study of the effects of live roots on rill erodibility in a field plot study using corn and soybeans. Semicircular rills, 5.3 m long and 63.5 mm deep were constructed in freshly tilled, fallow, corn, and soybean plots. Rill cross section and wetted area were measured over time with an imaging device and a pin profiler for five different flow rates, ranging from 7.57-37.85 L/min, at three different crop stages. Erosion rates, soil strength, root length density, soil aggregate stability, and carbon content were also measured. Soil erodibility and critical shear stress (K_d and τ_c) were determined by plotting the erosion rate versus the applied shear stress. Soil strength was over 20% greater under corn and soybeans than under fallow conditions. As with the laboratory study, the soil detachment rate was influenced by RLD, the stage of plant growth, and time. On average, D_r for corn and soybeans was 50% less than the D_r for fallow conditions. The authors showed that D_r decreased exponentially with increasing RLD. The exponents varied from -0.09 for corn to -2.3 for soybean, with r^2 of 0.14 - 0.54. This decrease in D_r with increasing RLD was attributed to the physical restraint of soil particles by roots. The presence of corn and soybeans roots also decreased K_d over 50%. As with the laboratory study, there was no correlation between τ_c and either K or D_r; τ_c decreased with both time and growth stage. This decrease in τ_c was attributed to small variations in detachment rates at low flows. While both aggregate stability and soil organic carbon content decreased under fallow conditions, both increased with increasing RLD, indicating the influence of roots on soil physical properties.

2.6.2.2. Effects of Roots on Soil Properties

Vegetation indirectly affects soil erosion by changing soil physical and chemical properties including soil organic matter, aggregate stability and bulk density (Mamo and Bubenzer, 2001a,b). While the effects of vegetation on soil structure is well known, the impacts have not been well quantified (Materechera et al., 1992). Reid and Goss (1980) evaluated the effects of ryegrass on the aggregate stability of a sandy loam. Ryegrass was grown in pots for four weeks and the aggregate stability of the planted pots was compared to fallow pots using turbidimetric analyses and wet sieving. Most of the roots were removed prior to testing by sieving the soil through a 4.0 mm mesh. Results showed that after only four weeks the ryegrass significantly increased aggregate stability, predominately for the larger aggregates. The authors attributed this increase in soil stability to root exudates. Since the pots were maintained at a

constant moisture content, soil consolidation due to WDC did not occur. Additionally, the researchers observed soil particles attached to plant mucilage around the root tips.

In a follow-up study, Reid and Goss (1981) investigated the effects of lucerne, maize, perennial ryegrass, tomato and wheat on the aggregate stability of both “fresh” and air-dried samples from two soils. A sandy loam and silt loam were sieved through a 2.0 mm mesh and placed in pots at a constant moisture content. The plant were only grown for periods of either 25 or 42 days, depending on growth rate, to minimize the effects of increases in organic matter from root decomposition on aggregate stability. Soils were maintained at a constant water content throughout the study. Using turbidimetric analyses and wet sieving, the aggregate stability of both fresh and rapidly air-dried soils were measured. Additionally, root length and weight, root hair length, and the degree of infection by mycorrhizal fungi were assessed. The results indicated the growth and activity of ryegrass and lucerne roots significantly increased aggregate stability. Increases in soil stability were attributed to polysacharide mucilages produced in the plant rhizospheres. No correlation between aggregate stability and root length or root hair length was shown. In contrast to the lucerne and ryegrass, the stability of fresh aggregates decreased under maize, tomato and wheat, although results were not conclusive for tomato or wheat. In contrast, the stability of air-dried aggregates under wheat was greater than the fallow controls. The authors suggest difference in aggregate stability resulted from variations in the polysaccharides produced by the five plant species.

Materechera et al. (1992) evaluated the effects of plants and WDC on aggregate formation in two agricultural soils in Australia. A loam and a hydromorphic clay were air-dried, ground, and sieved through a 0.5 mm mesh to destroy the existing macrostructure. Soil "minirhizotrons" were created and planted with pea, wheat and ryegrass. Unplanted minirhizotrons were used as controls. Designed as a 2x4x2 factorial experiment, half of the pots underwent 15 WDCs while the other half were maintained at constant moisture levels. The samples were maintained for four to seven months, depending on the length of time required to undergo 15 WDCs. Aggregate size distribution, aggregate stability (wet-sieving of air-dry samples), aggregate tensile strength, root length density, aggregate bulk density, and aggregate organic carbon contents were measured. Results of the study showed that RLD increased in the order of ryegrass>wheat>pea and that RLD was positively correlated to aggregate size distribution, stability, tensile strength, bulk density and organic carbon content. The effect of

plants on aggregate formation was attributed to increases in soil stress during root penetration, as well as chemical stabilization by the production of mucilage and the establishment of soil microorganisms. Multiple WDCs also produced significant aggregate formation through increases in soil tensile stress and soil cracking. While both plants and WDC were significant in the formation of soil aggregates, the authors felt changes in water regime were more important for aggregate formation than plants.

Haynes and Beare (1997) studied the effects of barley, wheat, prairie grass, Italian ryegrass, and two legumes, white clover and lupin, on soil organic matter and aggregate stability in a silt loam soil. Root mass and length, microbial biomass carbon, soil organic carbon, total and extractable soil carbohydrate content, bacterial number and fungal hyphae length were also measured. The six plant species were grown in pots for 12 weeks before sampling. The results showed that plants have a significant effect on aggregate stability and microbial biomass carbon, with microbial biomass and aggregate stability increasing with root length and root mass. Roots and fungal hyphae increase aggregate stability by creating a physical mesh that binds soil particles and by exuding polysaccharides and other organic substrates which act as soil glues. Additionally, increases in total root mass increase soil organic carbon, which in turn leads to an increase in soil microbes. Similar to plants, soil microbes influence soil stability by exuding polysaccharide and phenolic binding agents.

2.6.2.3. Root Density in Stream Banks

The influence of root density and vegetation type on the erosion of red clay soils in the western Lake Superior basin was investigated by Davidson et al. (1991). Root biomass was determined by excavating 0.5 m^2 quadrats in 10 cm increments to a depth of 0.5 m. Roots were separated into 10 diameter classes. In general, root mass in clay soil under forested vegetation had twice the root biomass as under herbaceous vegetation. Root distribution with depth was dependant on soil type: in clay soils most of the root biomass was found in the top 50 cm of the soil profile, while in sandy soils the roots extended to greater depths. Vegetation type also influenced root distribution. In clay soils, 90% of the herbaceous root mass was located in the upper 10 cm, as compared to 50% for woody vegetation.

Shields and Gray (1992) studied sand levees on the Sacramento River, California. Five sites with woody vegetation were compared to a herbaceous control. Root distributions were

measured for seven diameter classes using the profile wall method (Bohm, 1979). Root density decreased exponentially with root diameter. Average root area ratios (RARs) ranged from 0.001% to 2.02%, with an average of 0.17%. Root area ratio is the total root area per unit area of soil on a profile wall. The largest RAR was observed in the top 10 cm of the herbaceous control, although this was biased by the presence of a single large root. On average, 43% and 50% of the woody and herbaceous root area, respectively, occurred in the top 30 cm of the soil profile. At depths greater than 20 cm, there were no significant differences in RAR under woody and herbaceous vegetation. Herbaceous roots were short and oriented vertically. In contrast, woody roots radiated from laterally from the root crown, parallel to the ground surface. The authors noted that the woody roots generally angled downward and attributed this orientation to the droughty sandy soils.

The root distribution for two species of Australian riparian trees was investigated by Abernethy and Rutherfurd (2001). Root area ratio was measured along profile walls at varying distances from the tree thickets and at depths of 1 – 2 m. The RARs ranged from 0.001% to 0.756% and generally decreased with depth and distance from the trees. Some scatter occurred in the measurements made near the trees: RAR is biased by the presence of individual large roots.

Simon and Collison (2002) measured RAR for four common riparian tree species and two grass species in the Goodwin Creek Experimental Watershed in northern Mississippi. The trees ranged in age from 5 years to 12 years, while the grasses were 5 years old. Average RARs varied from 0.0056% to 0.012% for the trees and from 0.0044% to 0.014% for the grasses. While the RARs were similar for the trees and grasses, the number of roots per unit area was one to two orders of magnitude greater for the grasses than for the trees. The majority of the roots were small diameter: the tree roots were generally less than 2 mm in diameter and the grass roots were mostly smaller than 1 mm. The largest tree root diameters were 9 – 16 mm, while the largest grass roots were less than 3 mm in diameter. Roots were concentrated in the upper soil profile with 90% of the roots in the top 17 cm for eastern gamma grass (*Tripsicum dactyloides*), 32 cm for black willow (*Salix nigra*), 38 cm for sweetgum (*Liquidambar styroflora*), 56 cm for switch grass (*Panicum virgatum* ‘Alamo’), and 74 cm for sycamore (*Platanus occidnetalis*). The roots were generally oriented horizontally, except the switch grass roots, which were oriented vertically.

2.6.3. Mass Wasting

Researchers have found that woody and herbaceous roots significantly increased slope stability over bare conditions (Waldron and Dakessian, 1982; Gray and MacDonald, 1989; Shields and Gray, 1992). The root systems of woody and herbaceous plants act to stabilize banks by increasing soil shear strength (Wu and McKinnell, 1976; Murgatroyd and Ternan, 1983; Abernethy and Rutherfurd, 2001). Soils are strong in compression, but weak in tension; shear stress in the soil is transferred to tensile stress in the roots (Thorne, 1990; Langendoen, 2000). Even small increases in root density can substantially increase soil strength (Gray and MacDonald, 1989; Abernethy and Rutherfurd, 2001). Micheli and Kirchner (2002) measured a linear relationship between riparian meadow root biomass and soil shear strength, with riparian vegetation increasing soil shear strength as much as 800%.

Changes in soil strength are a function of root size, distribution, and tensile strength (Abernethy and Rutherfurd, 2001). Several researchers have found a nonlinear inverse relationship between root strength and root diameter (Waldron and Dakessian, 1981; Abernethy and Rutherfurd, 2001; Simon and Collison, 2001). Large roots (> 15– 20 cm in diameter) do little to increase shear strength, but instead act as soil anchors (Simon and Darby, 1999). Additionally, the stems of woody plants act as soil buttresses and arches, further protecting banks against mass failure (Abernethy and Rutherfurd, 1998). In a study of two different tree species, Abernethy and Rutherfurd (2001) determined root strength was unrelated to species or test method. Roots typically fail by tensile or bond failure, although scour of exposed roots also occurs (Wu, 1984; Thorne, 1990; Abernethy and Rutherfurd, 2001). The ability of roots to resist pullout is a function of root length, branching patterns, root tortuosity, and soil type (Abernethy and Rutherfurd, 2001).

Tengbeh (1993) studied the effect of perennial ryegrass roots (*Lolium perenne*) and soil moisture content (MC) on soil shear strength. Both a sandy clay loam and a clay were dried and sieved in 2 mm sieve. The soils were planted at different densities (100, 190, 380 seeds/m^2) and grown in a greenhouse for different periods of 4 - 30 weeks. Soil shear strength was measured with a hand-held direct vane shear tester, while root density was quantified by sampling root biomass. The results of the study showed that soil shear strength of both rooted and unrooted samples increased exponentially as the soils dried. The rate of change in shear strength with MC was greatest for rooted soils at low moisture contents. Roots increased shear strength by at least

500% for the sandy clay loam and up to 850% for clay at MC near saturation. Additionally, the rooted soils attained a maximum shear strength at a lower MC than root-free soils. The authors attributed these findings to root exudates, suggesting that the root exudates helped bind the soils. The MC of maximum strength for the rooted soils was well below the soil plastic limit; therefore, the concept that the maximum shear strength occurs at the soil plastic limit may not apply to rooted soils. Because the amount of reinforcement provided by the roots varied with soil texture, the authors questioned the accuracy of bank stability models that assume increases in soil cohesion due to roots are a function of root density only.

2.6.4. Benefits of Herbaceous vs. Woody Vegetation

As discussed in the Introduction section, there is considerable debate in the literature regarding the relative merits of herbaceous versus woody riparian vegetation (Lyons et al., 2000; Simon and Collison, 2001). With regard to subaerial processes, Stott (1997) found that soil temperature and moisture regimes were moderated by forest cover, as compared to moorland vegetation. Soil temperature in the forest was an average of 3.7ºC higher. As a result, stream banks with forested riparian buffers may experience fewer WDCs or FTCs.

Both herbaceous and woody vegetation provide increased hydraulic roughness, although the effects of herbaceous vegetation are reduced at high flows because grasses and forbs bend over in the flow. Additionally, herbaceous vegetation is absent or reduced during the winter when most channel erosion occurs. As a result of reduced stream width, velocities in grass channels have been found to be greater than those with forested vegetation (Horwitz et al., 2000)

In addition to hydraulic effects, vegetation type appears to influence stream sediment regime. Bedload transport rates under forested buffers are 2 - 6 times those measured under herbaceous buffers (Murgatroyd and Ternan, 1983; Stott et al., 1986; Kirby et al., 1991; Reed, 1999). Reed (1999) attributed this difference to a greater water surface slope in forested sections and increased sediment storage in grassed reaches.

Herbaceous vegetation has a greater density of fine roots, as compared to woody vegetation (Tufekcioglu et al., 1999). This high root density will likely produce greater τ_c and shear strength under herbaceous vegetation. Several authors claim stream channels are narrower with grass buffers because the grass acts to armor stream banks and trap fine sediments (Murgatroyd and Ternan, 1983; Sweeney, 1993; Trimble, 1997b; Davies-Colley, 2000; Lyons et

al., 2000; Simon and Collison, 2001); however, bank reinforcement extends only to the rooting depth (Thorne, 1990). While trees have fewer fine roots, they also have a greater rooting depth (Gregory and Gurnell, 1988). Davidson et al. (1991) determined that 50% of tree roots and 90% of grass roots were located in the top 10 cm of clay soils in Minnesota and Wisconsin. As a consequence, undercutting of grass banks is commonly observed (Davies-Colley, 1997). Most tree and shrub roots are found in the top 50 cm of soil (Jackson et al., 1986; Sun et al., 1987; Tufekcioglu et al., 1999; Simon and Collision, 2001). Abernethy and Rutherfurd (2000) observed little root growth where river banks were permanently saturated. This may be particularly significant in headwater areas where groundwater is shallow, making trees vulnerable to windthrow (Abernethy and Rutherfurd, 1998).

Waldron (1977), Waldron and Dakessian (1981; 1982) and Waldron et al. (1983) conducted a series of experiments comparing the shear strength of grass, legume, and tree roots. They ultimately concluded that woody roots provided greater strength and were more effective for soil stabilization. This conclusion has been supported by some researchers (Beschta and Platts, 1986; Johnson et al., 2001) and refuted by others (Murgatroyd and Ternan, 1983; Trimble, 1997b; Lyons et al., 2000).

2.7. Summary

Because riparian vegetation has a significant impact on stream stability and morphology, it has become an integral part of stream restoration designs. Currently, designs are based on empirical methods and standardized practices, which do not permit the assessment of designs for long term stability in the face of future landuse change (Henderson, 1986; Gregory and Gurnell, 1988; O'Laughlin, 1995; Shields, Jr. et al., 1995; FISRWG, 1998; Jennings et al., 1999; Horwitz et al., 2000; Hession, 2001). Additionally, as states are required to develop management plans with TMDLs for listed impaired waters, there will be a need to quantify all significant sources of sediment within watersheds and to determine the effect of proposed controls. To improve stream restoration design and riparian management, a better understanding of the effects of vegetation on the processes involved in stream bank retreat is necessary (Abernethy and Rutherfurd; 1998).

The impacts of vegetation on stream bank stability are complex, poorly understood, and have yet to be quantified (Thorne et al., 1997; ASCE, 1998a; Abernethy and Rutherfurd, 2000). Vegetation influences the chemical and physical properties of stream banks, as well as the local

microclimate. Long term, continuous records of stream bank soil moisture and temperature regimes are necessary to determine the effects of vegetation on subaerial processes (Thorne et al., 1997). Also, little quantitative information is available on the effects of vegetation on stream bank scour (Smith, 1976; Kamyab, 1991; Dunaway et al., 1994). It is believed the root systems of woody and herbaceous plants physically and chemically bind bank soils in place (Gray and Leiser, 1982; Coppin and Richards, 1990; Thorne et al., 1997). Allen et al. (1997) noted that the presence and density of roots seemed to influence soil erodibility, but the effect of roots on the stream bank erodibility and critical shear stress have not been investigated, to the authors knowledge.

The overall goal of this study is to evaluate the effect of vegetation on the erosion of stream banks. Specifically, this study will focus on the influence of roots on the fluvial entrainment of stream bank soils. Because subaerial processes are responsible for making soils more vulnerable to erosion, their effects will also be considered. The effects of vegetation on mass wasting will not be addressed for multiple reasons. First, the analysis of mass wasting involves complex geotechnical slope stability assessments that are beyond the current knowledge of the author. Second, this aspect of bank erosion is currently being addressed by several researchers (Simon et al., 2000; Abernethy and Rutherfurd, 2001; Simon and Collison, 2001). Third, few design data exist on the erosion of stream bank sediments and there is even less information on the effect of vegetation on this process. Lastly, mass wasting is inextricably linked with fluvial entrainment; therefore, an improved understanding of the effects of vegetation on the fluvial entrainment of soils is required to improve predictions of stream bank erosion. Ultimately, this research seeks to answer the following questions:

1. What is the density and distribution of roots within stream banks, as a function of aboveground vegetation density and type?
2. How does riparian vegetation affect subaerial processes?
3. Does vegetation have a significant impact on the fluvial entrainment of stream banks soils, in comparison to other soil properties?
4. Can the erodibility and critical shear stress of rooted stream banks soils be predicted using the parameters measured in this study?